FANO RESONANCE FILTERS ON PATTERNED SILICON PHOTONIC CRYSTAL NANOMEMBRANES

by

SANTHAD CHUWONGIN

Presented to the Faculty of the Graduate School of

The University of Texas at Arlington in Partial Fulfillment

of the Requirements

for the Degree of

MASTER OF SCIENCE IN ELECTRICAL ENGINEERING

THE UNIVERSITY OF TEXAS AT ARLINGTON

December 2008

Copyright © by Santhad Chuwongin 2008

All Rights Reserved

ACKNOWLEDGEMENTS

I am grateful to all people who helped and inspired me during my master study program and made this thesis possible. I appreciate very much the advice and help from the my thesis committee members, Profs. W. D. Zhou, J. C. Chiao, M. Vasilyev, N. Stelmakh, and M. Lu.

Especially, I would like to express my profound appreciation to my master supervisor Prof. Weidong Zhou with his support, assistance, suggestions, and encouragement helping me all the time during my research and study at The University of Texas at Arlington. He was always influenced and willing to help his advisees with their research. His persistent energy and enthusiasm had motivated all students and post doctors in our group. Therefore, this thesis became true and rewarding to me.

I would like to thank the support from members of Dr. Zhou's Nanophotonic Device Research Group. Special thanks to Dr. Zexuan Qiang for device simulation and design, Hongjun Yang and Li Chen for the help on the device fabrication and testing.

I would like to thank the Nanafab, the nanotechnology research and teaching facility, for giving me the most useful equipments. I also have to thank all research engineers who gave me the training, suggestion, and help at Nanofab.

I am thankful to The Royal Thai Government who gave me a chance to study aboard and provided me the whole financial support during my study.

I would like to thank my parents Mrs. Ratchanee Kuawong, Mr. Vinai Chuwongin, and my mother-in-law Mrs. Sommai Chomwan who raised me with the lovely warm and I wish them have to be in good health. Lastly, I am thankful to my wife Mrs. Dararat Chuwongin who encourage me to finish this thesis earlier and support me everything.

November 21, 2008

ABSTRACT

FANO RESONANCE FILTERS ON PATTERNED SILICON

PHOTONIC CRYSTAL NANOMEMBRANES

SANTHAD CHUWONGIN, M.S.

The University of Texas at Arlington, 2008

Supervising Professor: WEIDONG ZHOU

Recently broadband reflectors and guided-resonance narrowband filters have been proposed to be the major components in communication and optical interconnect systems. Most work reported so far are based on free-standing membranes. Recent advances in the fabrication process have made it possible to pattern crystalline silicon nanomembranes (NMs) and transfer to foreign substrates. These NMs are transferable, stackable, bondable and manufacturable. In this thesis, we present two-dimensional photonic crystal broadband reflectors and narrowband filters based on Fano resonances on patterned silicon nanomembranes, on Si, glass, and polyethylene terephthalate (PET) substrates. For broadband reflectors, spectral trimming was achieved by partially or even completely removing the buried oxide layer (BOX) on silicon-on-insulator (SOI), by controlling SiO_2 thin film deposition or spin-on-glass coating surrounding the silicon nanomembranes. Resonance tuning was demonstrated with a turning range over 50 nm for both blue- and red-shifts, making it a practical design tool for Fano resonance trimming for both narrow band filters and ultra-compact broadband reflectors. For narrowband filters, the characteristics of Fano filters based on transferred silicon nanomembranes on PET and glass substrates are reported. Both experimental and theoretical analyses were performed on angular- and polarization-dependent transmission properties.

TABLE OF CONTENTS

LIST OF ILLUSTRATIONS

LIST OF TABLES

Table Page

CHAPTER 1

OVERVIEW OF FANO RESONANCE

A two-dimensional photonic crystal slab (2D-PCS) is a slab structure with periodic refractive index modulation in two-dimensions and homogeneous index distribution in the third dimension, as shown schematically in Figure 1.1. The periodic refractive index modulation leads to the formation of discrete guided mode in plane[12] If a forbidden region is formed over a range of frequencies for all in-plane directions, photonic bandgap appear in the plane of periodicity, or appear in the plane of discreteness, or in-plane. On the 3rd dimension in PCS, the refractive index differences lead to the formation of lightline, where only those modes lie below the lightline can be confined within the slab (in-plane guided modes).[4] On the other hand, there are other modes that differ from guided modes since such these modes which occur above the light-line ($\omega(k) \geq ck/n$) can couple light inside the slab to the external surrounding, and these modes are called “radiation modes”. By taking these helpful properties so called “Fano resonance”, narrowband filters and broadband reflectors usually investigated the reflection and transmission spectra that interact between the radiation modes and external incident light can be established.

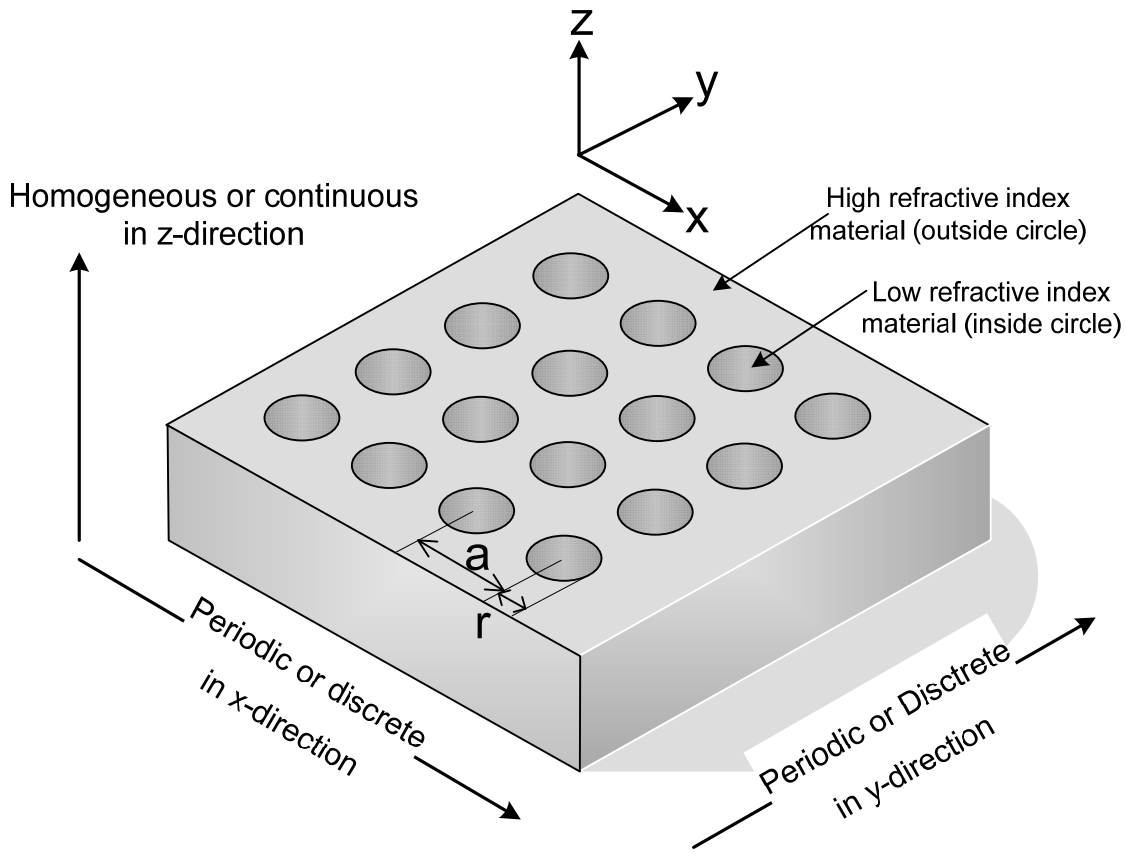

Figure 1.1 Schematic of two-dimensional photonic crystal silicon nanomembranes.

1.1 Fano resonance principle

The Fano resonance (or Guided Mode Resonance, GMR) phenomenon is manifested by the presence of a discrete state (in plane guided resonant mode) strongly coupled with a continuum of states (out-of-plane or vertical radiation modes) as shown in Figure 1.2 due to phase matching provided by the periodic lattice structure so that the guided radiation mode can provide an efficient way to channel light from within the slab to the external environment, and vise versa.[2,4] Fano resonance plays an important role in filters and reflectors design since it has useful characteristics as follows: First, photonic bandgaps is not required because these modes operate above light-line ($\omega(k) = ck/n$) or outside bandgaps which is defined as the boundary of the gray area in Figure 1.2 . Second, the difference between low and high dielectric indices can

be relaxed. Lastly, the design for both high Q filters and broadband reflectors on the resonance is flexible.[2,3]

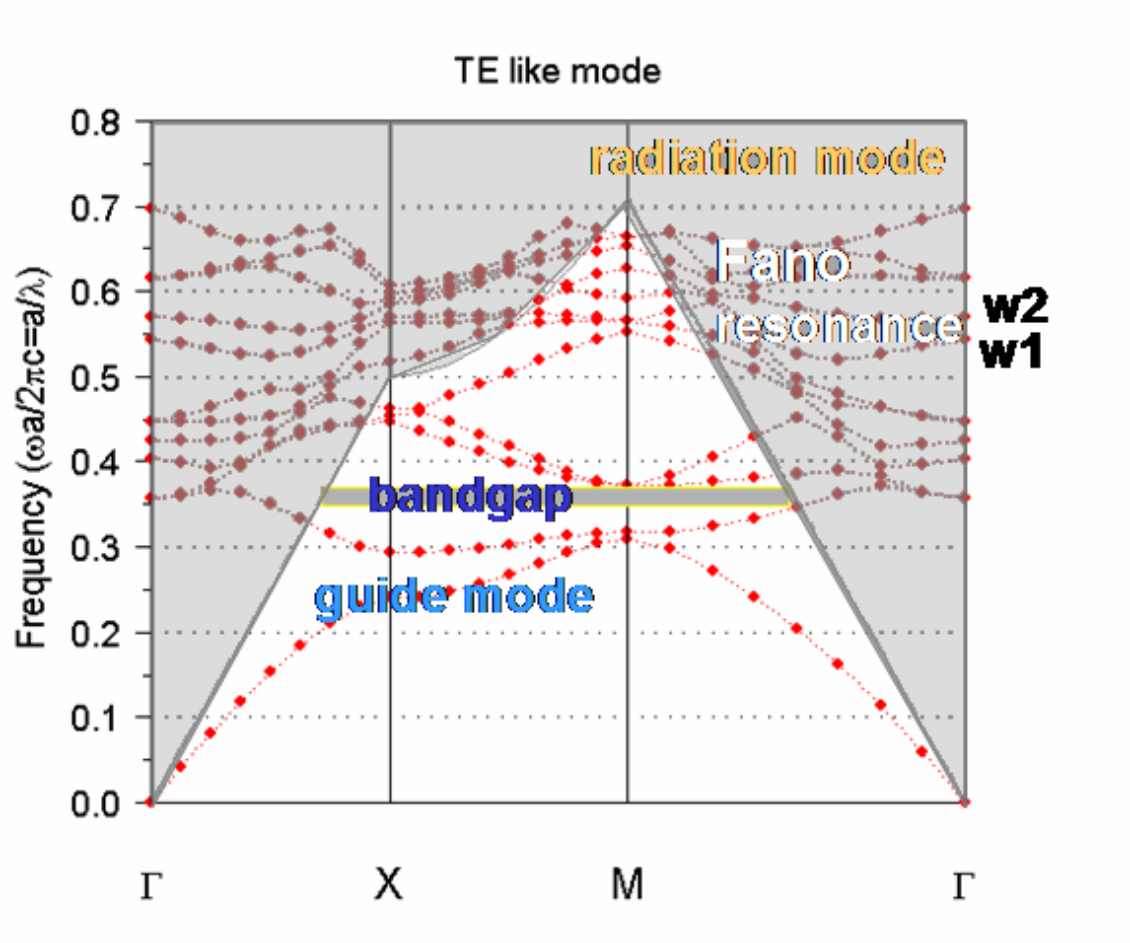

Figure 1.2 Guided modes below light line confined in the slab and radiation modes above light line radiated without any restriction in the vertical direction.

1.2 Fano resonance for filter devices

When the uniform dielectric slab without photonic crystal structures was characterized, the transmission or reflection spectra with a frequency-dependent dielectric constant will have no sharp resonance.[4] whereas the low index material was introduced into high index material like in Figure 1.1 so that the 2D-PC was performed, the transmission and reflection spectra are similar to Fabry-Perot oscillation when incident light interacts with a uniform dielectric slab.[4] Therefore, in plane guided mode with periodic structures like multi-layer of infinite low refractive index or low dielectric constant and high refractive index or high dielectric constant strongly coupled with the out-of-plane guided mode resonance (GMR) will appear. Consequently, incident light will be strongly confined within the slab as shown in Figure 1.3 (left side) which is on resonance.[1] On the other hand, for off resonance mode, the distribution of power density will not be confined in the slab so that it radiates into air medium.[1]

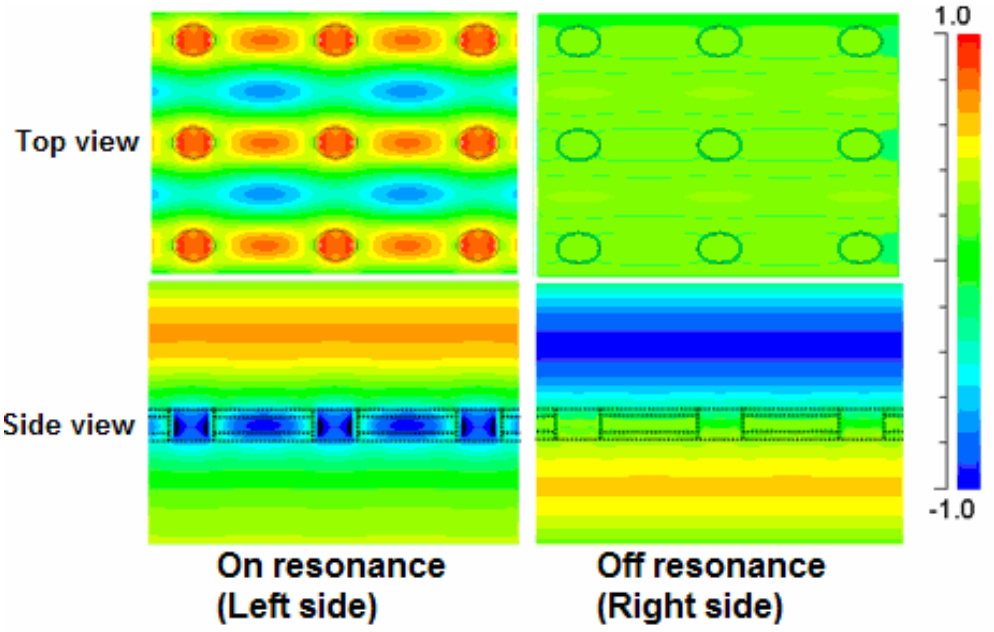

Figure 1.3 (Left side) Top view and side view of distribution of power density during on resonance. (Right side) Top view and side view of distribution of power density during off resonance.[1]

1.3 Design parameters for Fano devices

First, Starting material is Silicon-on-insulator (SOI) wafer with silicon top layer thickness 0.26 μm. SOI was chosen since it has buried oxide layer that will support Si top layer after SiNMs fabrication. Second, for two-dimensional photonic crystal filters, the design parameters are lattice constant (a), r/a where r is air hole radius, and t/a where t=thickness of silicon top layer. Finally, letting defined three types of different slab configurations as ASO (Air-Si-Oxide), ASA (Air-Si-Air), and OSO (Oxide-Si-Oxide) are selected for convenience as shown in Figure 1.4. From Figure 1.8, the design parameters are a=0.8 μm; r/a=0.25; t/a=0.425 when reducing the oxide thickness from 0.34 μm to 0.1 μm the spectral peak shifts to the left which is shorter wavelength, and with the same parameters as in Figure 1.5, further keep reducing the oxide thickness, the spectra further shifts toward shorter wavelength. If the oxide layer below slab was completely removed, the spectral peak will cease at about 1.35 μm as shown in Figure 1.6.

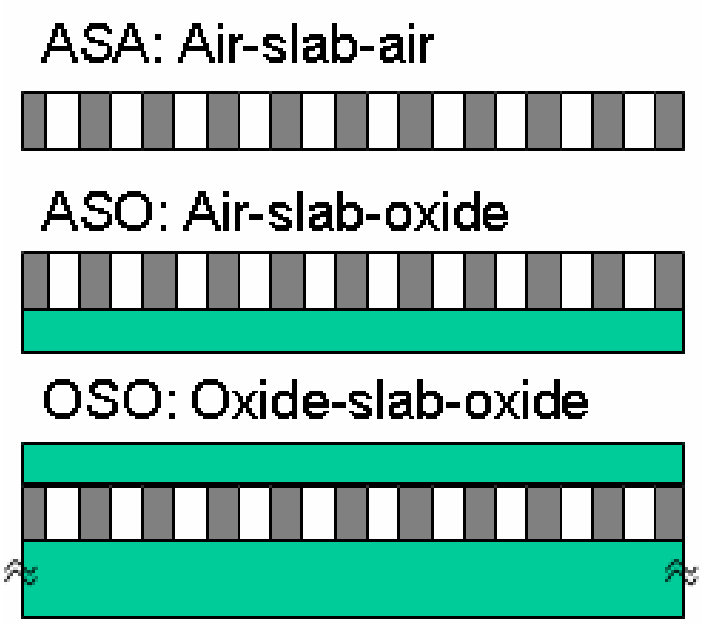

Figure 1.4 Three types of different slab configurations.

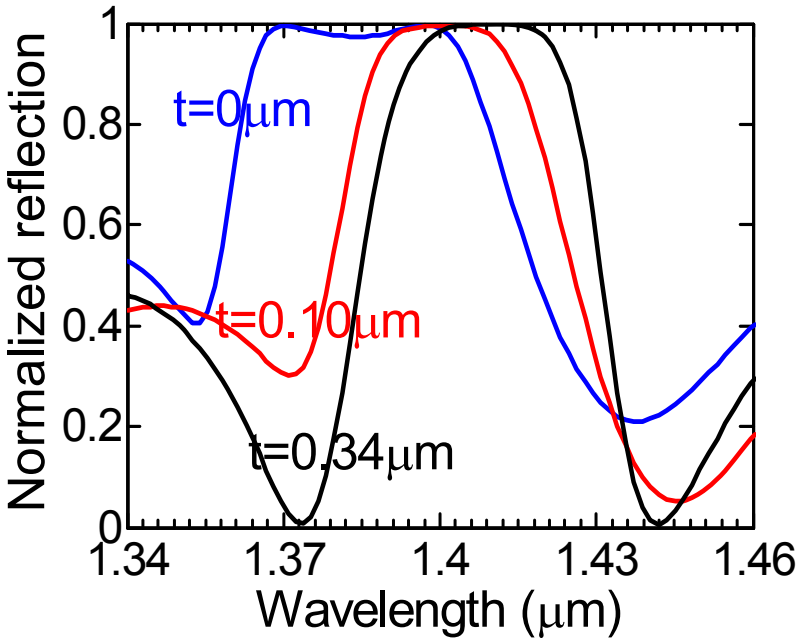

Figure 1.5 Impact of oxide thickness on filter design when reducing from 0.34 to 0.1 μm.

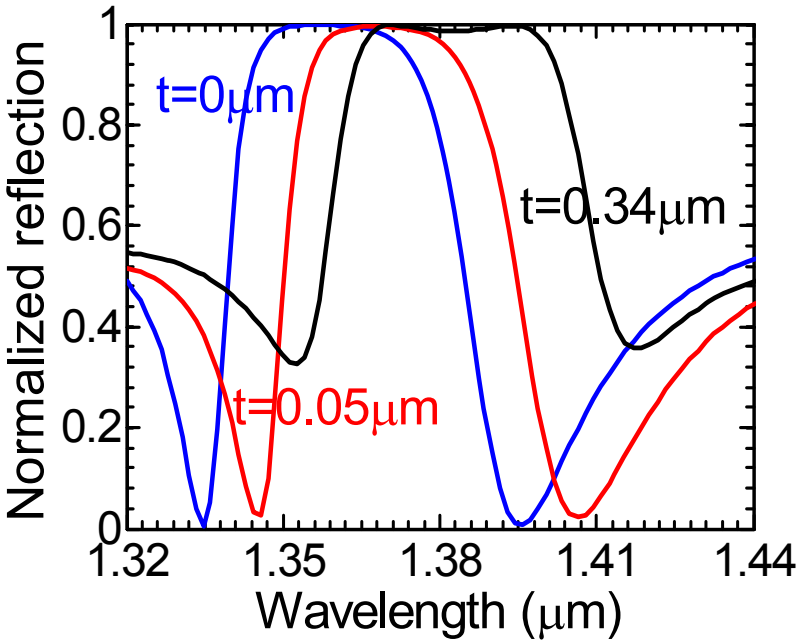

Figure 1.6 Impact of oxide thickness on filter design when reducing from 0.34 to 0.05 μm.

By increasing lattice constant a and r/a from 0.8 μm to 0.85 μm and from 0.25 to 0.26 respectively for all types of different configurations, the broadband reflection spectra can be obtained, and all spectral peaks shift toward the longer wavelength as shown in Figure 1.7 and 1.8. After the lattice constant was increased, a little broadband spectra can be achieved, however, the parameter r/a need to be increased as well.

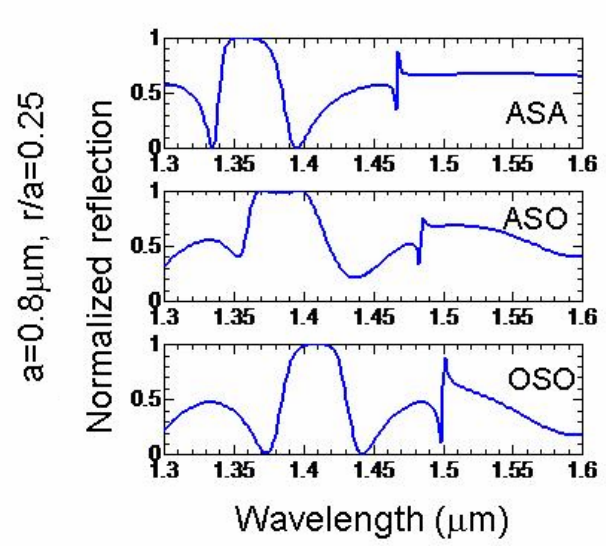

Figure 1.7 Impact of oxide for design parameters a=0.8μm, r/a=0.25.

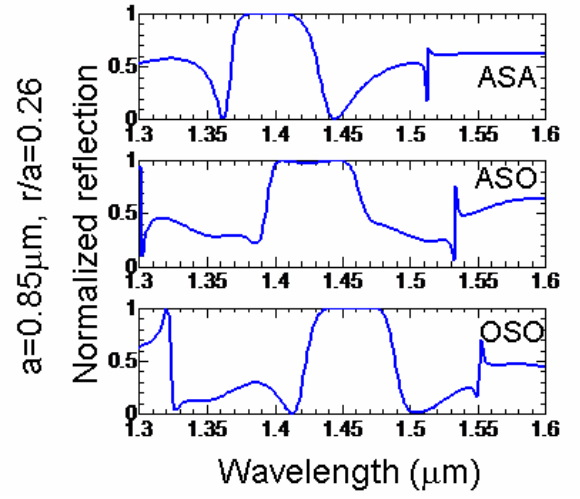

Figure 1.8 Impact of oxide for design parameters a=0.85μm, r/a=0.26.

In order to optimize broadband spectral reflection, we keep increasing lattice constant a and r/a from 0.9 μm to 0.95 μm and from 0.26 to 0.265 respectively for all types of different configurations. Similarly, the broadband reflection spectra can be obtained very well, and all spectral peaks shift toward the longer wavelength as shown in Figure 1.9 and 1.10. With the increase of lattice constant, more and more large flat bandwidth can be succeeded and flat spectra will shift towards longer wavelength.

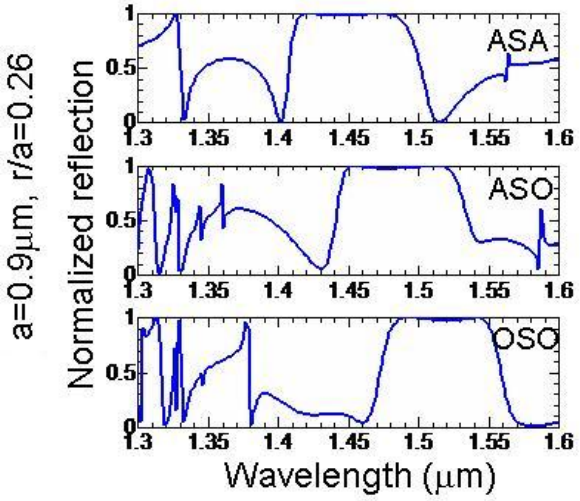

Figure 1.9 Impact of oxide for design parameters a=0.9 μm, r/a=0.26.

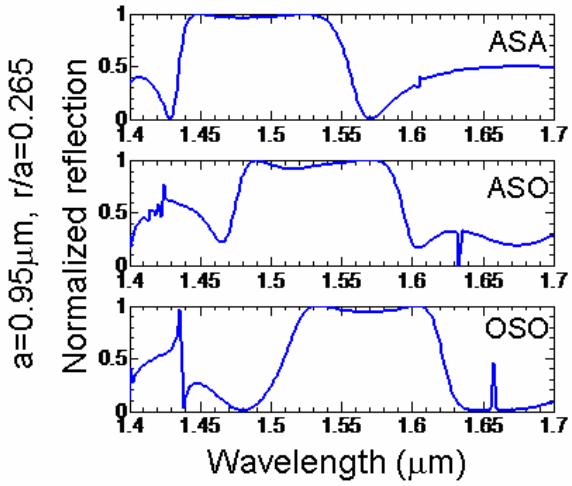

Figure 1.10 Impact of oxide for design parameters a=0.95 μm, r/a=0.265.

Keeping further optimized parameters to obtain very broadband spectra by increasing lattice constant to 1 μm so that r/a need to be increased to 0.265 as well in order to achieve large broadband spectra. From Figure 1.11, the large broadband spectra can be obtained as expectation, however, spectra ripple in the middle band of spectra rises up and more and more high order modes will appear in the short wavelength. The Fano devices fabrication design with different configurations and different parameters are shown in table 1.1.

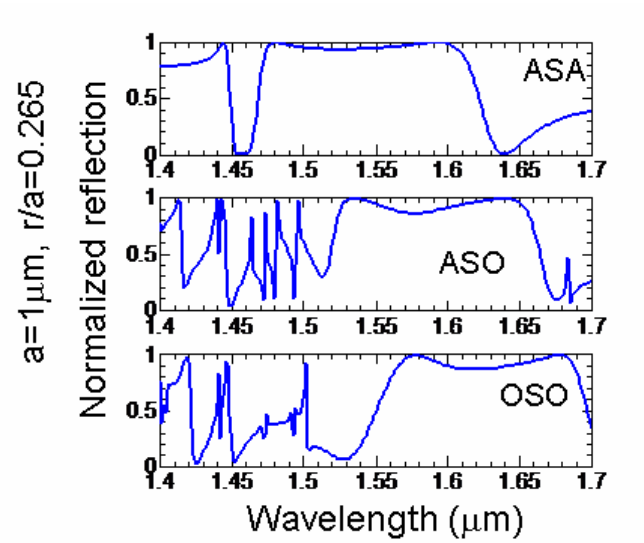

Figure 1.11 Impact of oxide for design parameters a=1 μm, r/a=0.265.

Table 1.1 Summary for Fano device design with Si top layer 340 nm thickness for different configurations

No.	a (nm)	r/a (nm)	Config.	96% BW1	96% BW2	Mid. point	BW (nm)	Center (nm)	BW (%)
1	800	0.25	ASA	1346	1372	100	26	1359	1.91
	800	0.25	ASO	1368	1402	97	34	1385	2.45
	800	0.25	OSA	1366	1400	98	34	1383	2.46
	800	0.25	OSO	1398	1422	100	24	1410	1.70
2	850	0.26	ASA	1375	1418	100	43	1397	3.08
	850	0.26	ASO	1400	1454	96	54	1427	3.78
	850	0.26	OSA	1400	1449	97	49	1426	3.44
	850	0.26	OSO	1432	1479	98	47	1456	3.23
3	900	0.26	ASA	1416	1486	98	70	1451	4.82
	900	0.26	ASO	1448	1522	96	72	1485	4.98
	900	0.26	OSA	1444	1516	96	74	1480	4.86
	900	0.26	OSO	1482	1550	97	68	1516	4.49
4	950	0.265	ASA	1441	1538	96	97	1490	6.51
	950	0.265	ASO	1484	1580	92	96	1532	6.27
	950	0.265	OSA	1480	1570	93	90	1525	5.90
	950	0.265	OSO	1524	1610	94	86	1567	5.49
5	1000	0.265	ASA	1474	1602	93	128	1538	8.32
	1000	0.265	ASO	1528	1650	89	122	1589	7.68
	1000	0.265	OSA	1520	1642	86	122	1581	7.72
	1000	0.265	OSO	1570	1684	86	114	1627	7.01

CHAPTER 2

FABRCATION OF FILTERS AND REFLECTORS

After photonic crystal (PC) patterns were fabricated on silicon-on-insulator (SOI) wafer using e-beam lithography technique and reactive-ion etching (RIE) process. Then, the spectral trimming can be accomplished with the post-process control of the buffer layer index above and below the PC patterned silicon nanomembranes (SiNMs), with two different techniques . The first approach is to deposit SiO2 dielectric thin film on top of the patterned SiNMs by PECVD or spin-on-glass coating processes. Due to the addition of SiO2 layer on top, the effective index of the buffer layer increases, which lead to spectral shift towards longer wavelength (red-shift). The second approach is to selectively remove the buried oxide (BOX) layer with controlled wet etching by employing buffered hydrofluoric acid (BHF). In this case, the resonance spectral location will shift towards shorter wavelengths (blue-shift). Depending on the applications, the fabricated filters and reflectors can also be transferred to other foreign substrates such as glass or plastic substrates. By employing the wet-transfer process, the PC patterns were successfully released onto supported material substrate.[8]

2.1 E-beam lithography and dry etching

Silicon-on-insulator (SOI) is used as the starting material, with top Si layer thickness 270nm, and buried oxide (BOX) thickness 3 μm on Si substrate. E-beam lithography is an attractive technique for fabricating the two dimensional SiNMs on the SOI wafer by employing an electron beam to expose high resolution positive resist (ZEP520A). Then, an HBr/Cl_2 chemistry based reactive-ion etching (RIE) process is applied. In order to simplify the transmission and reflection measurement, the large area (~5x5 mm^2) of the high quality uniform pattern photonic crystal SiNMs was fabricated since a light beam spot can be easily aligned to the patterned photonic crystal SiNMs during testing as shown in Figure 2.1. Practically, the patterned SiNMs area is

approximately ten times of lattice constant (a), or only has ~5x5 μm^2 to ~10x10 μm^2 for devices with an operation wavelength of 1550 nm. The scanning electron micrograph (SEM) of the large area SiNMs patterns (~5x5 mm^2) is also partially shown in Figure 2.2.

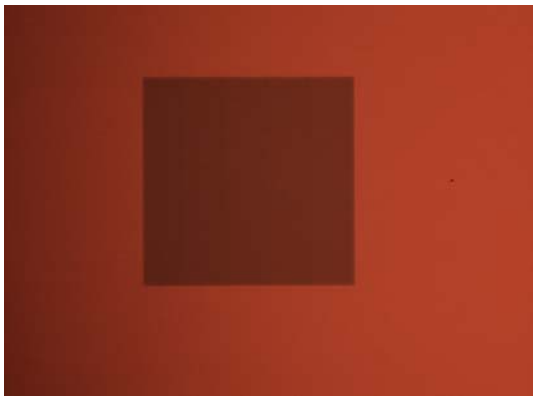

Figure 2.1 Photonic crystal SiNMs with patterned area ~5x5 mm^2.

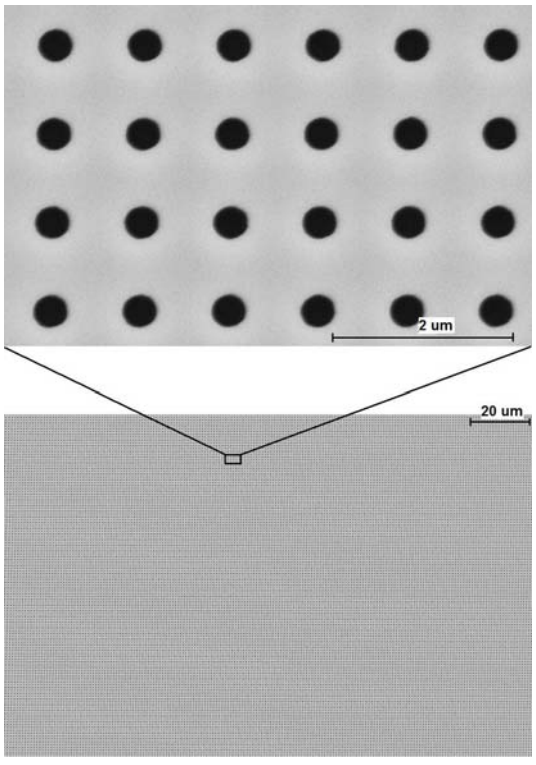

Figure 2.2 An SEM image of photonic crystal SiNMs with patterned area ~5x5 mm^2.

2.2 Wet-transfer technique

Silicon nanomembranes (SiNMs) on SOI substrate can be transferred onto flexible PET plastics or glass substrates[3], using wet–transfer process[8] at low temperature. The SOI wafer was immersed in aqueous diluted hydrofluoric acid (HF) solution (49% HF: DI water = 1:4) for several hours to etch buried oxide (BOX) layer from SiNMs selectively. When the BOX layer was completely removed, the SiNMs was totally released. Then, it was rinsed by DI water and transferred onto PET or glass substrates[7] as demonstrated in Figure 2.3. In this technique, the optional SU8 coating on glass may be applied to improved adhesion and mechanical stability for our devices[1] as shown in Figure 2.4. It can be clearly seen that the high quality transferred SiNMs structure can be obtained when it was verified with diffraction pattern measurements[1] as demonstrated in Figure 2.5.

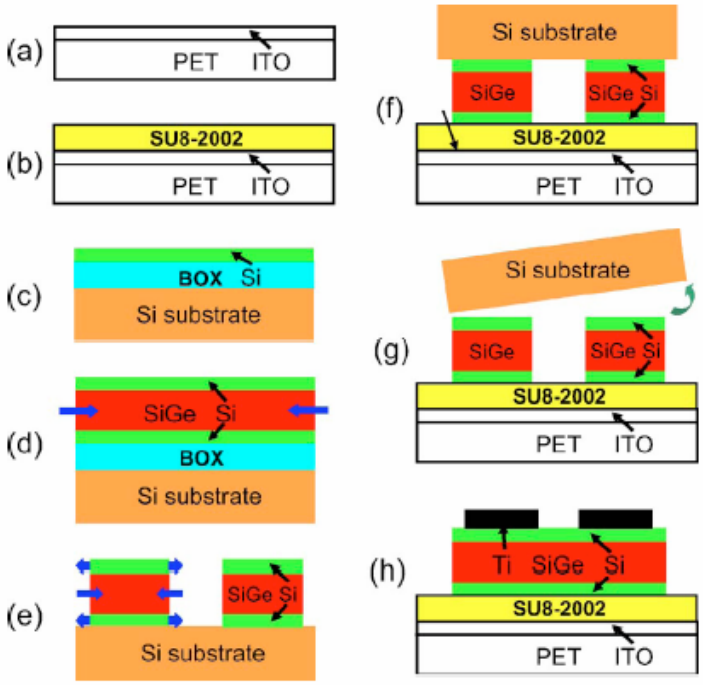

Figure 2.3 Wet-transfer processes starting from (a) to (h) to transfer patterned Si to foreign substrates.[7]

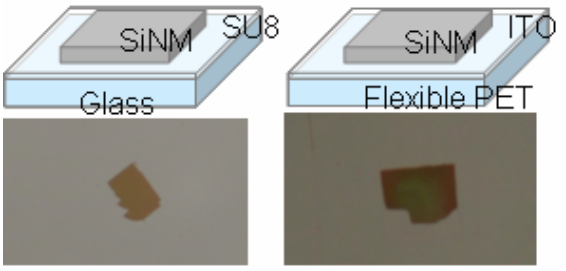

Figure 2.4 The SU8 coating on glass applied to improved adhesion and mechanical stability.[1]

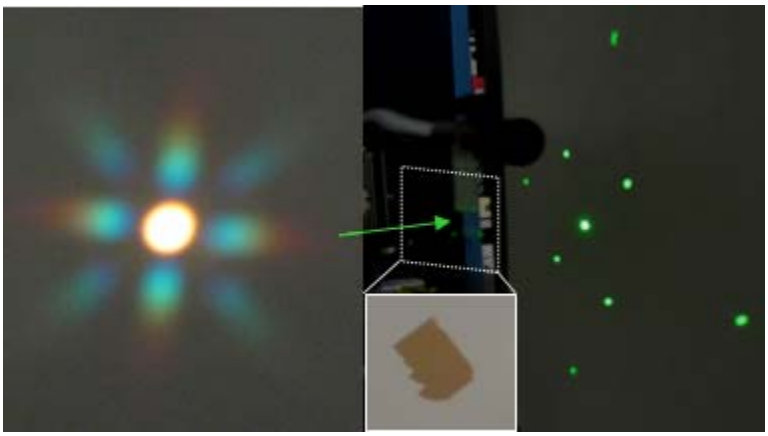

Figure 2.5 The uniform diffraction pattern obtained with broadband QTH lamp (right) and green laser (left) aligned on devices.[1]

2.3 Wet etching (BHF) for spectral trimming

Initially, the original PC structure on SOI wafer is shown in Figure 2.6. In order to remove silicon dioxide layer, buffered hydrofluoric acid (BHF) can be used since BHF etches silicon dioxide film much faster than it etches silicon nanomenbrances, and this process is performed by immersing the small wafer SiNMs in the solutions. The etching rate is around 100nm of oxide/minute at 25 C. After wet etching two minutes, buried oxide under SiNMs was partially and completely removed when it was immersed into the BHF solution seven minutes as shown in Figure 2.7 and 2.8 respectively because of the isotropic wet chemical etching profile, thus the reflection spectra can be shifted toward the shorter wavelengths so called “Blue-shift” as demonstrated in Figure 2.9 and 99% reflection spectral widths for different PECVD oxide

thickness starting from 0 to 298 nm shown in Figure 2.10. In Figure 2.11 (a) (b), shown the reflection spectra shifted to shorter wavelengths due to BHF process from 1 minute to 7 minutes.

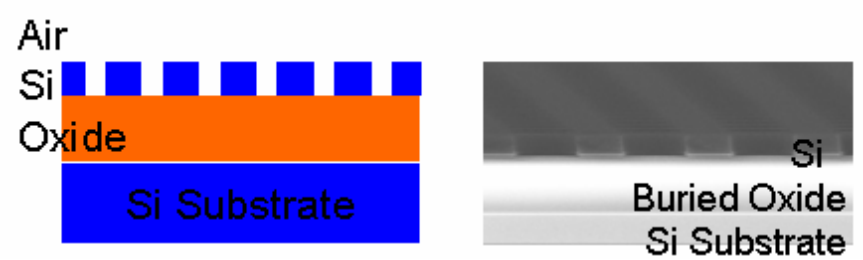

Figure 2.6 Original PC structure defined as ASO (Air-Si-Oxide).

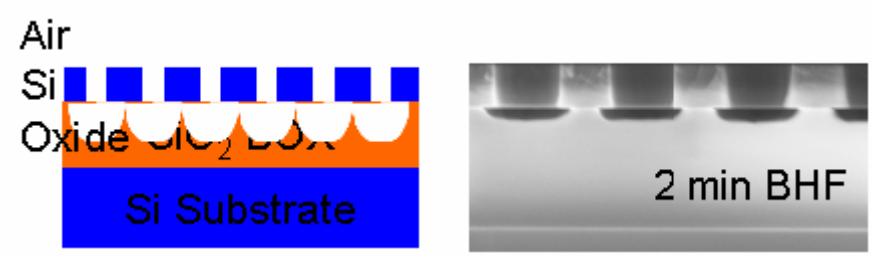

Figure 2.7 BOX oxide was partially etched defined as ASO (Air-Si-Oxide) due to BHF 2 min.

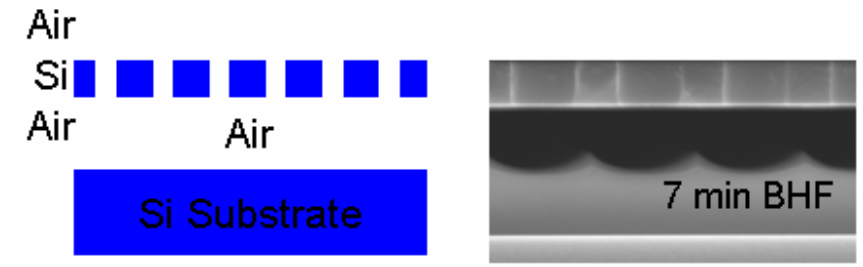

Figure 2.8 BOX oxide was completely etched away from SiNMs defined as ASA (Air-Si-Air) due to BHF 7min.

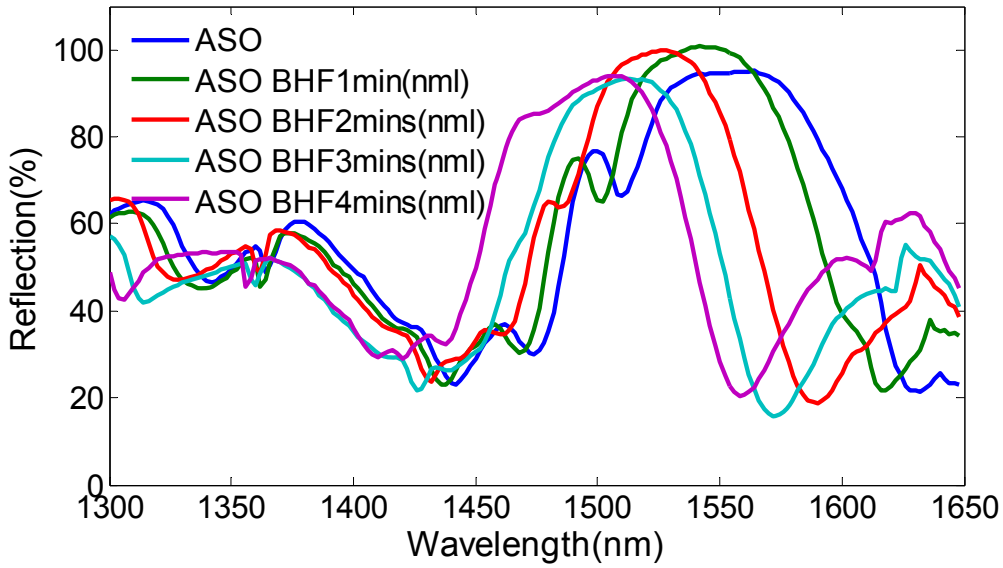

Figure 2.9 The reflection spectra shifted toward shorter wavelength "Blue-shift" due to partially buried oxide was etched.

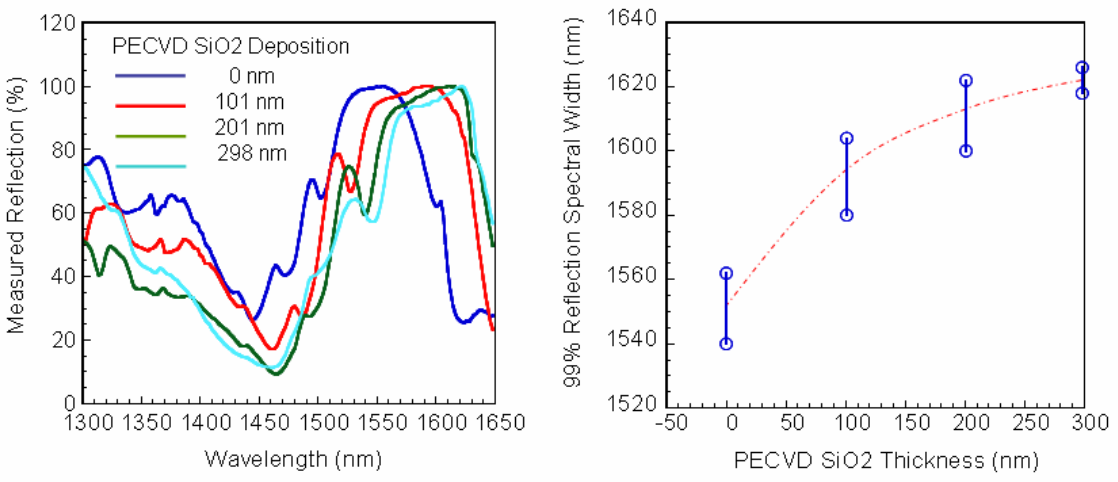

Figure 2.10 99% reflection spectral widths for different PECVD oxide thickness.[3]

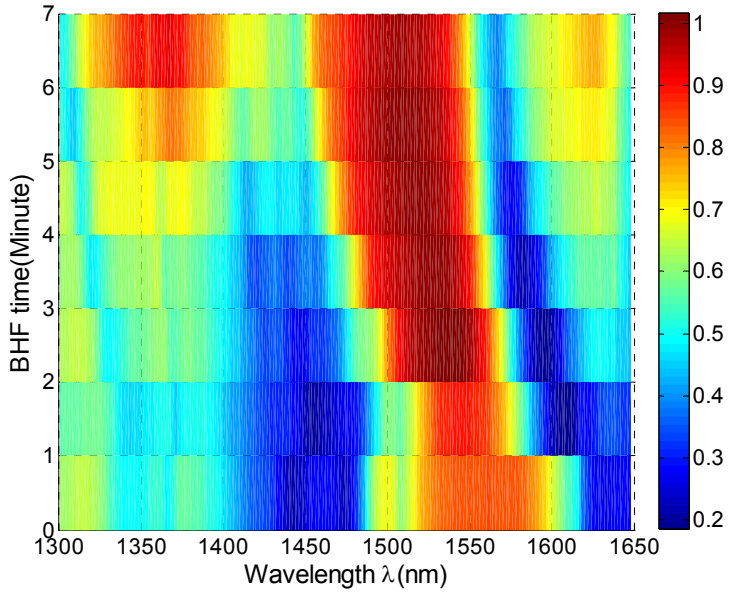

(a)

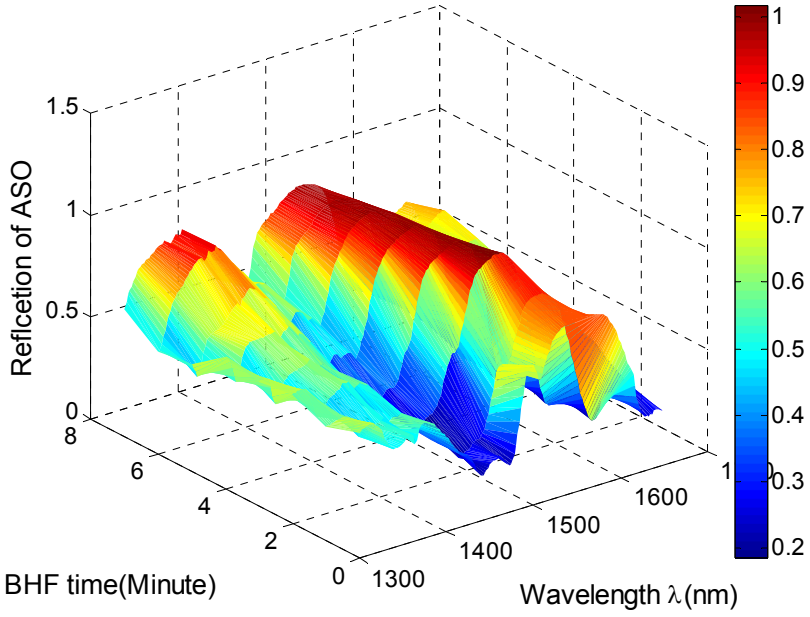

(b)

Figure 2.11 Three-dimensional spectrum of reflection spectra (a) top view (b) isotropic view.

Buffered Oxide Etch (BOE) or Buffered Hydrofluoric acid (BHF) is applied for removing SiO_2 layer from devices so as to move the reflection spectra from longer wavelengths toward shorter wavelengths so called “Blue-shift”. In our case, the spectral peaks value were intentionally place at the target wavelength 1.55 μm which is the near IR communication region. BOE etching solutions are composed of water 40-70%, Ammonium Fluoride (NH_4) 30-50%, and Hydrogen Fluoride (HF) 0.5-10%. Since NH_4 and HF can cause poisoning, anyone who uses these etchant mixtures must wear lab protective equipment such as goggles and shield, lab coat and apron, and proper gloves. The SEM image of SiNMs structure after BHF etching is shown in Figure 2.12.

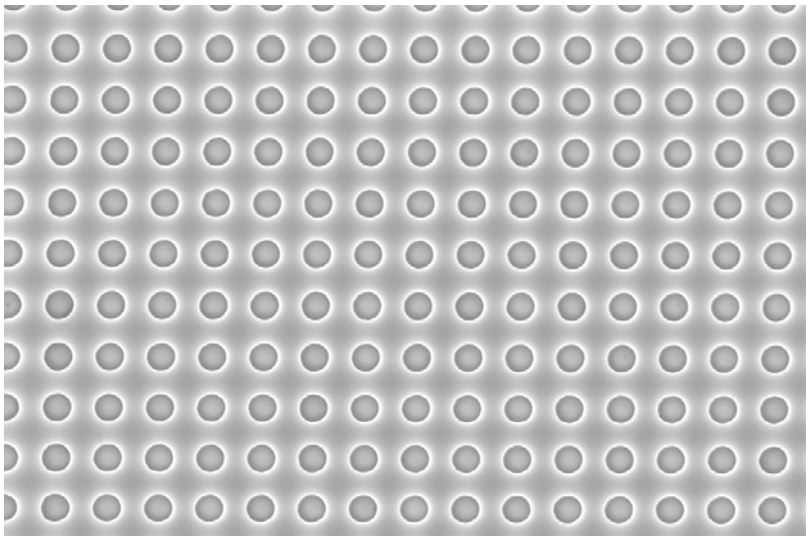

Figure 2.12 An SEM image of SiNMs after BHF wet etching.

2.4 Silicon dioxide deposition for spectral trimming

2.4.1 PECVD

Silicon dioxide layer can be uniformly deposited on silicon nanomembranes (SiNMs) in order to tune the reflection spectra to the longer wavelengths so called “Red-shift” as shown in Figure 2.13 when comparing with the original spectra. Silicon Oxide(SiO_2)thin films are deposited by PECVD (Plasma-Enhanced Chemical Vapor Deposition) at low temperature 200

°C -350 °C using radio frequency energy to generate highly reactive ions in the plasma systems as shown in Figure 2.14 and radical ions from plasma bombard the wafer surface to create silicon oxide layer. For oxide deposition, Silane (SiH_4) and Nitrous oxide (N_2O) are used:

$$3SiH_4 + 6N_2O \rightarrow 3SiO_2 + 4NH_3 + 4N_2$$

In our process, the recipe SiO_2 –Nanofab –Deposition with non-uniformity <1% was used and the details are shown below.

Step 1:

Pressure	:	900 mTorr
ICP Power	:	75 mW
RIE Power	:	30 mW
Temperature	:	200 degree C
Time	:	100 seconds
N2O	:	160 sccm
N2	:	225 sccm
SiH4/Ar	:	24 sccm

Step 2:

Pressure	:	250mTorr
Temperature	:	200 degree C
Time	:	180 seconds
N2	:	250 sccm

The schematic of SiNMs after PECVD, and also SEM image are shown in Figure 2.15. The deposition rate that obtained from this recipe is about 74 nm per minute which is almost linear as plot in Figure 2.16 so that the SiO_2 thickness can be easily calculated by deposition time.

The SEM images of both PECVD SiO_2 100nm and 400nm are demonstrated in Figure 2.17 and 2.18 respectively. The spectral trimming can be done by adding the oxide surrounding the PC Si nanomembranes.

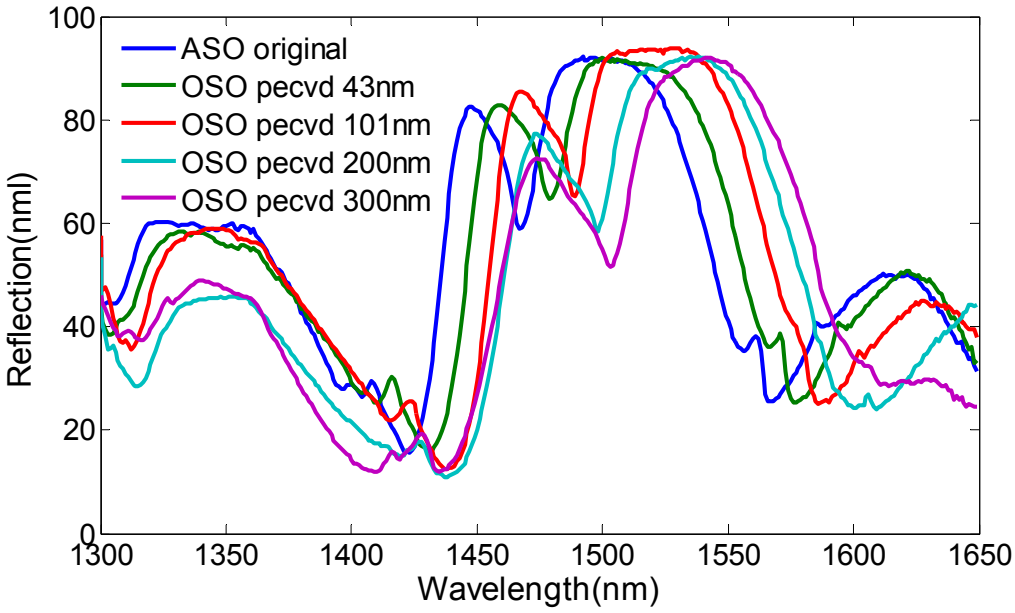

Figure 2.13 The reflection spectra shifted toward longer wavelength “Red-shift” due to PECVD SiO_2 deposition.

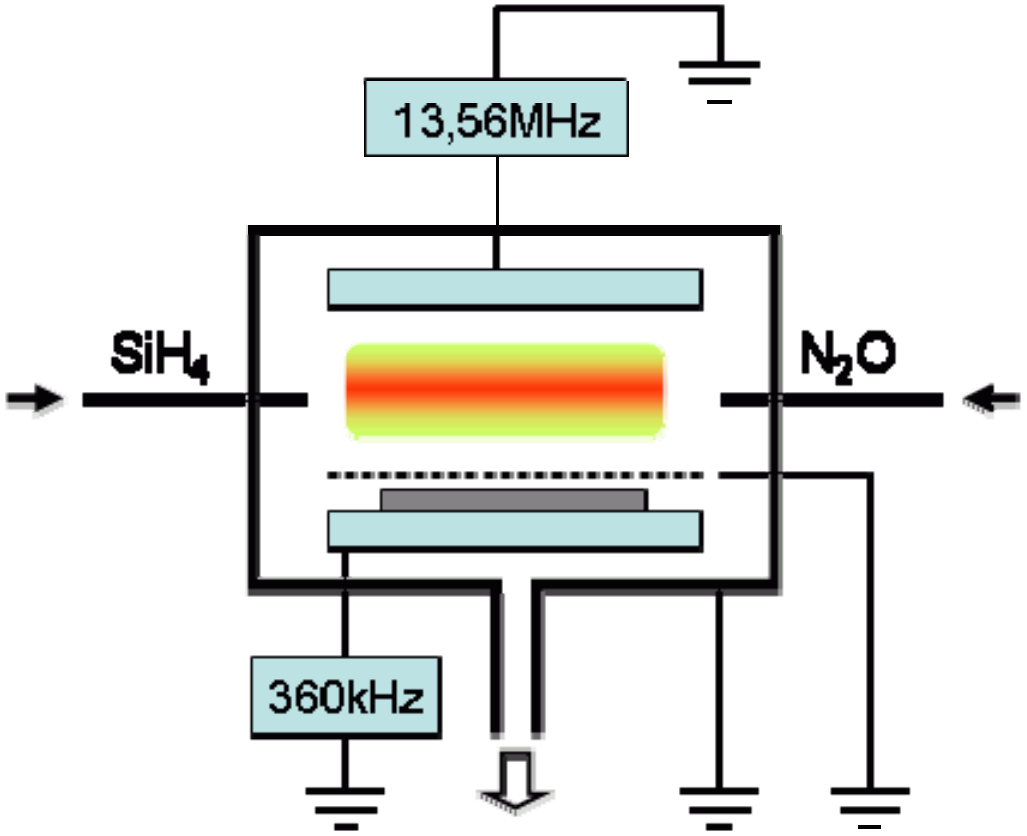

Figure 2.14 PECVD reactor.[9]

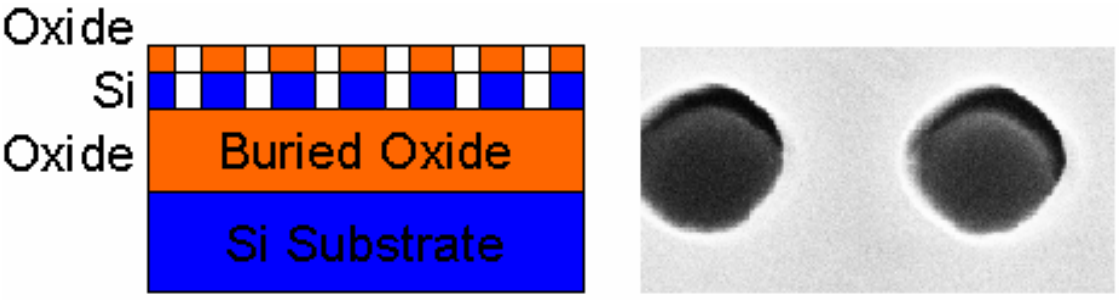

Figure 2.15 Oxide layer was deposited on top of SiNMs after PECVD.

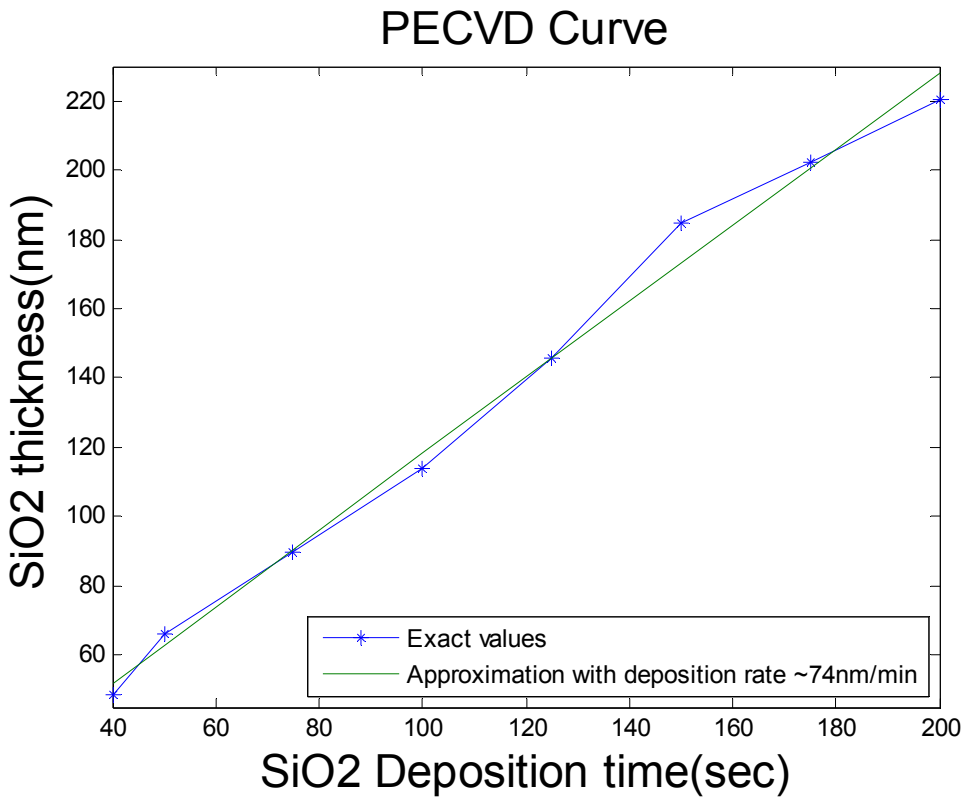

Figure 2.16 The deposition rate in PECVD obtained from experiments.

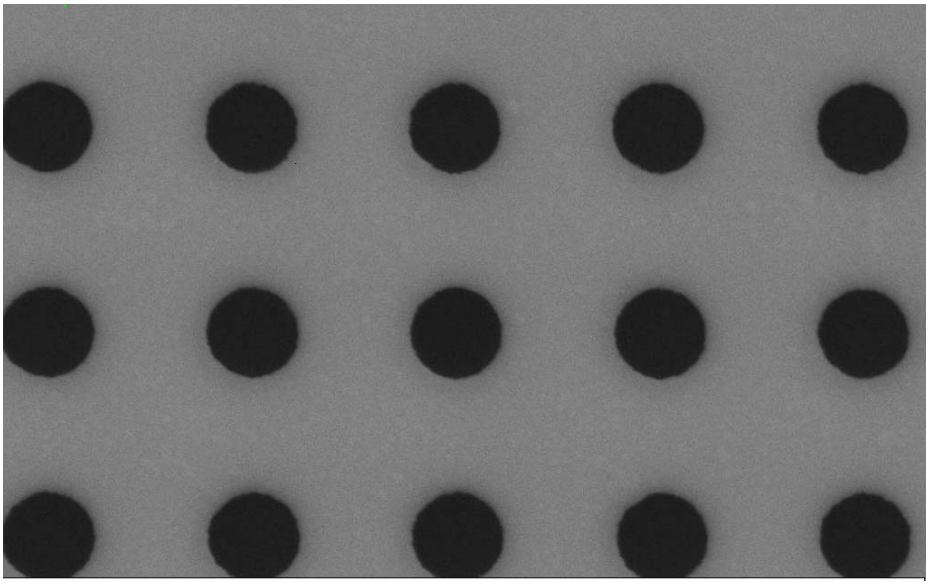

Figure 2.17 An SEM image of SiNMs after PECVD SiO_2 100nm thickness.

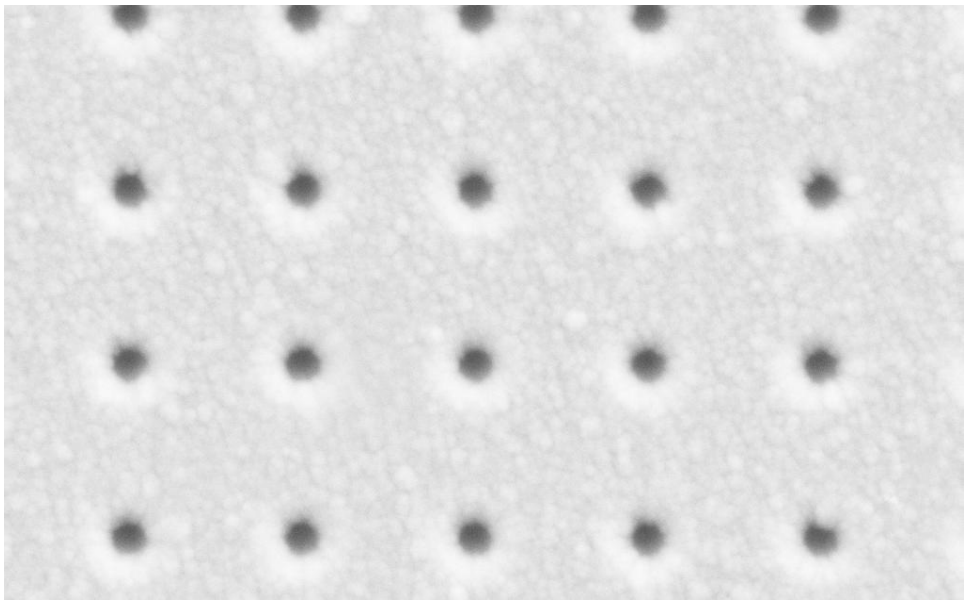

Figure 2.18 An SEM image of SiNMs after PECVD SiO_2 400nm thickness.

2.4.2 Spin-on-glass

By applying Spin-on-glass (SOG) P-112A (Phosphosilicate spin-on glass) which has low viscosity and good adhesion to the Spinner Headway, SiO_2 thin films can be performed good uniformity on top of SiNMs. The spectral trimming by SOG is the same as that by PECVD since the purpose of adding SiO_2 layer is required. However, the results are quite different as plotted in Figure 2.19 because of SOG backfilling of air region above, below, and in the air hole of patterned SiNMs as shown in Figure 2.20, on the other hand, PECVD deposition of SiO_2 on top of patterned SiNMs . The SOG thin films have the relation with the spin speed as plotted in Figure 2.20.

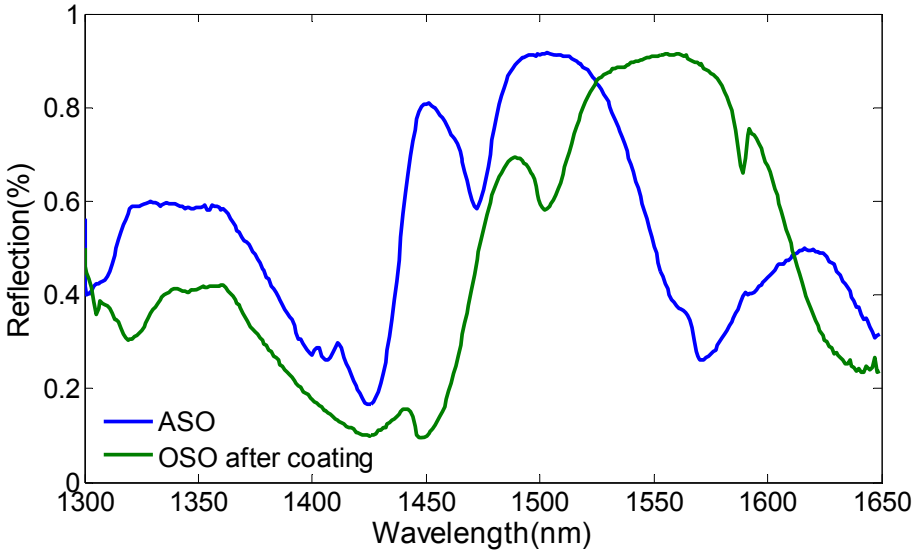

Figure 2.19 The spectral trimming of SiNMs having SOG backfilling.

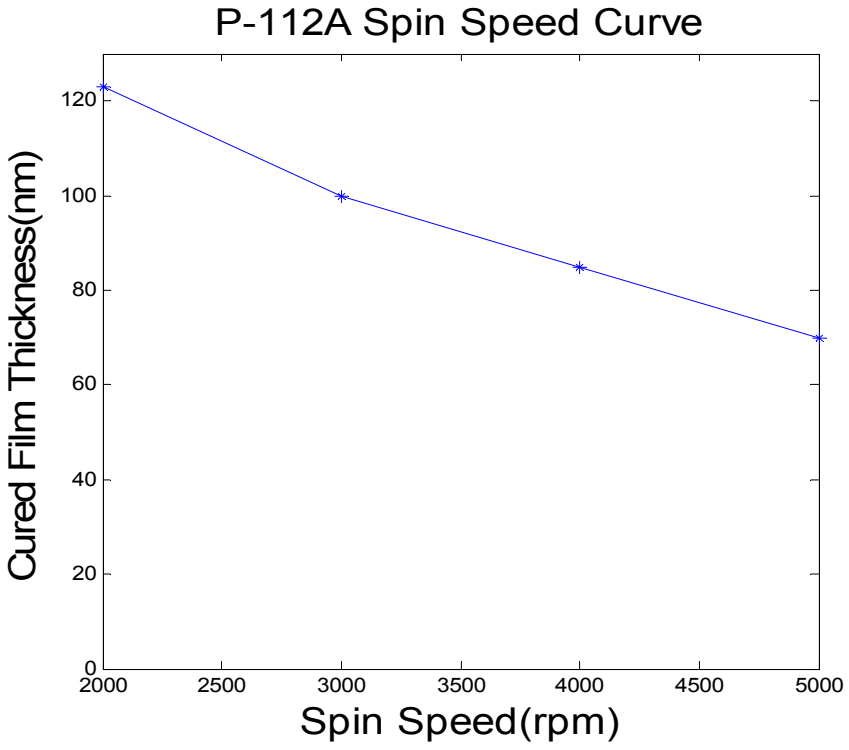

Figure 2.20 An SEM image of SiNMs after PECVD SiO_2 400nm thickness.

CHAPTER 3

MEASUREMENT SETUP AND RESULTS

After the devices were fabricated and transferred to the foreign substrate, they will be examined in order to compare between the simulation results and the measurement results, and both results ought to agree each other. In addition to transmission and reflection measurement, sometimes the process of transfer SiNMs is not perfect so that the diffraction pattern of devices needs to be investigated as well. In the end of this chapter, the SEM images are also shown to check the physical profile in nano-scale. Finally, the explanations of labview program that play an important role in measurements are also provided in detail.

3.1 Measured and simulated results

Finite difference time-domain (FDTD) and rigorous coupled-wave analysis (RCWA) play an important role in transmission and reflection property simulations, The structural design is based on plane-wave expansion (PWE) technique for dispersion plot simulation. For FDTD, plane wave source with two monitors is used including perfectly matched layer (PML) and periodic boundary condition (PBC) with single unit cell simulation. For RCWA, every structure created is three-dimensional structure and assuming in-plane is infinite and periodic. For convenience, will denoted the acronym for the SiNMs structure as follows: firstly, ASO is SiNMs surrounded by air (top) and oxide (bottom). Secondly, ASA is SiNMs surrounded by air on top and bottom. Thirdly, OSO is SiNMs surrounded by oxide on both top and bottom.

3.1.1 Narrowband filters

For narrowband filters transferred onto glass substrate, the design parameters have lattice constant (a) = 0.9 μm, r/a = 0.22, and t/a = 0.29 are considered. The simulated and measured transmission spectra are plotted in Figure 3.1.[1] Both results agree very well with each

other, especially at the target wavelength 1.551 μm. In this simulation, assuming the glass substrate has 5a thickness.

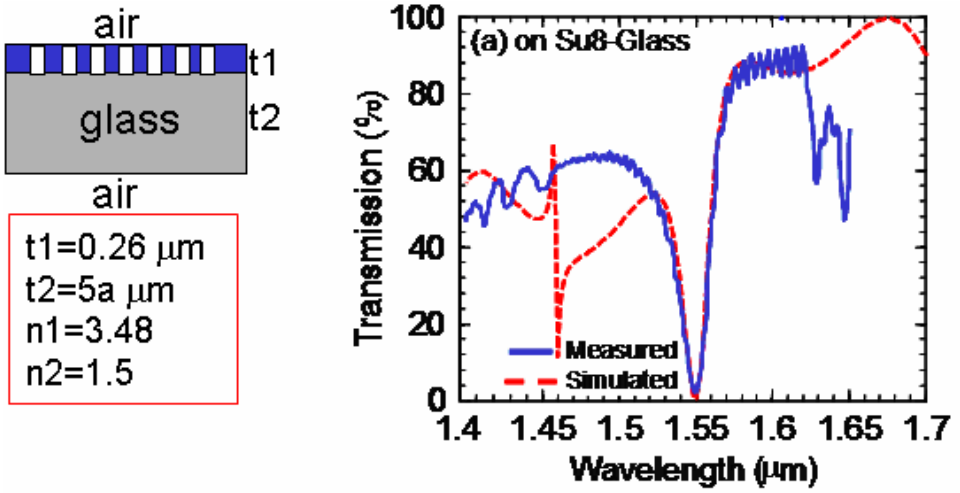

Figure 3.1 Simulated and measured transmission spectra of Fano filter on glass substrate.[1]

For narrowband filters transferred onto ITO-PET substrate, the design parameters have lattice constant (a) = 0.6 μm, r/a = 0.19, and t/a = 0.43 are considered. The simulated and measured transmission characteristics are shown in Figure 3.2.[1] The measured result agree well with simulated result that has dip locations at wavelengths 1.562 μm and 1.42 μm.

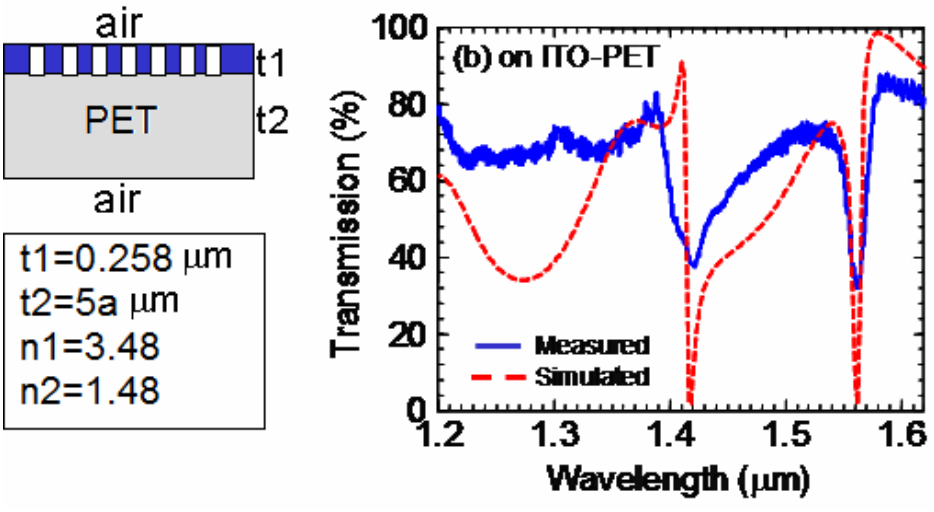

Figure 3.2 Simulated and measured transmission spectra of Fano filter on PET substrate.[1]

3.1.2 Broadband reflectors

In this section, the simulated and measured reflection spectra of different filter configurations are compared. Figure 3.3 shows three types of configuration filters. First, ASO original filter was fabricated on SOI. Second, ASA original filter was immersed into BHF 4 minutes to remove BOX oxide. Last, OSO original filter was deposited SiO_2 surrounding SiNMs with SOG backfilling. In Figure 3.4, ASO configuration filter was matched with simulated result. In Figure 3.5, ASA configuration filter was fitted with simulated result. In Figure 3.5, OSO configuration filter was compared to simulated result. After all measured and simulated results are matched there are some differences probably because of imperfect fabrication, unequal BHF, and non-uniform SOG backfilling respectively.

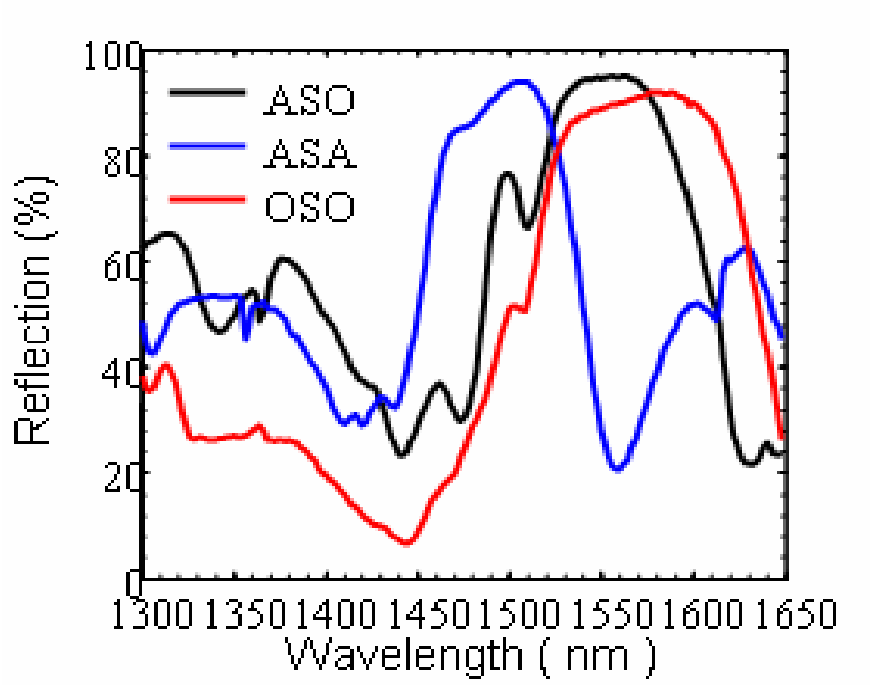

Figure 3.3 Measured reflections for three different configurations ASO, ASA, and OSO. [3]

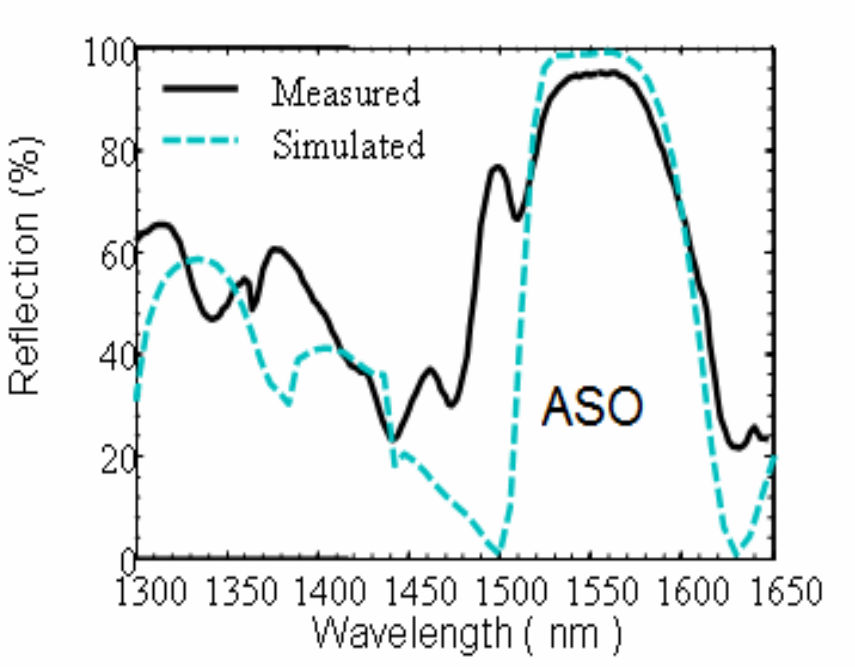

Figure 3.4 Measured reflections for ASO comparing to simulated result.[3]

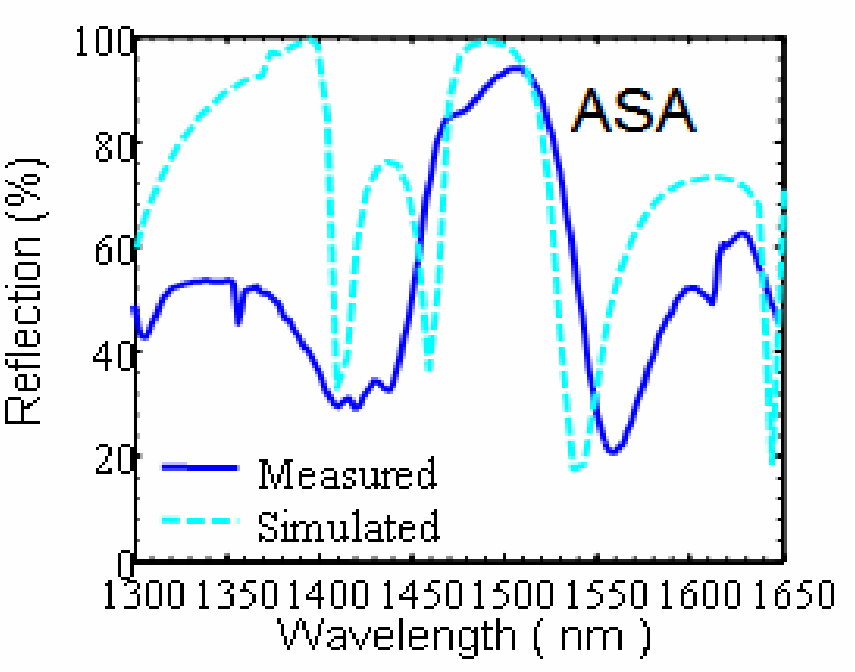

Figure 3.5 Measured reflections for ASA comparing to simulated result. [3]

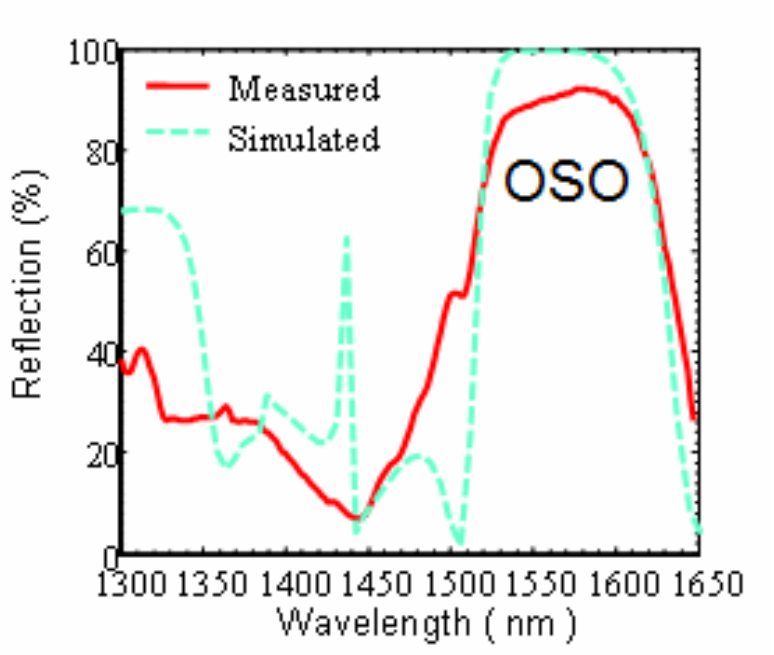

Figure 3.6 Measured reflections for OSO comparing to simulated result.[3]

3.2 Transmission and reflection measurement

For broadband reflectors, the reflection spectra will be obtained to characterize the properties of these reflectors, and the design parameters such as lattice constant (a) and airhole radius (r) are focused on the region starting from 1300 nm to 1650 nm which is inside infrared region (IR) and peak spectrum at wavelength operation of 1550 nm. The schematic of reflection measurement is demonstrated in Figure 3.7. Based on reflection setup, the device and the broadband metallic protected gold mirror used as a reference are mounted on the sample holder which can be moved freely in three-dimensional (3D) directions in order to control focused beam light on the patterned area. First, pointing focused beam of light source which is broadband quartz tungsten halogen (QTH) on the broadband metallic protected gold mirror until obtaining maximum sensitivity at lock-in amplifier by adjusting the 3D sample holder. Then, the reflection spectra of a reference will be measured by using labview program as shown in Figure 3.8. Second, when focused beam light gets through the iris diaphragm which is

opened as a small spot then passes through the beamsplitter and objective lens, beam light spot will focus on a reference and bounces off the beamsplitter then pass through the focal lenses which have big and small ones to focus light into the spectrometer following the beam light passes through a chopper in order to take the continuous wave of broadband light source and chop it up to higher frequencies. From there the light goes through the spectrometer slit which can be set to be narrow to reduce noises. Third, at the exit of the spectrometer, the signal is detected by the InGaAs IR detector. The signal detected by InGaAs IR detector will go to a lock-in amplifier. Consequently, the chopper frequency can be matched to that of the signal. Then it is rolled back to the labview program.

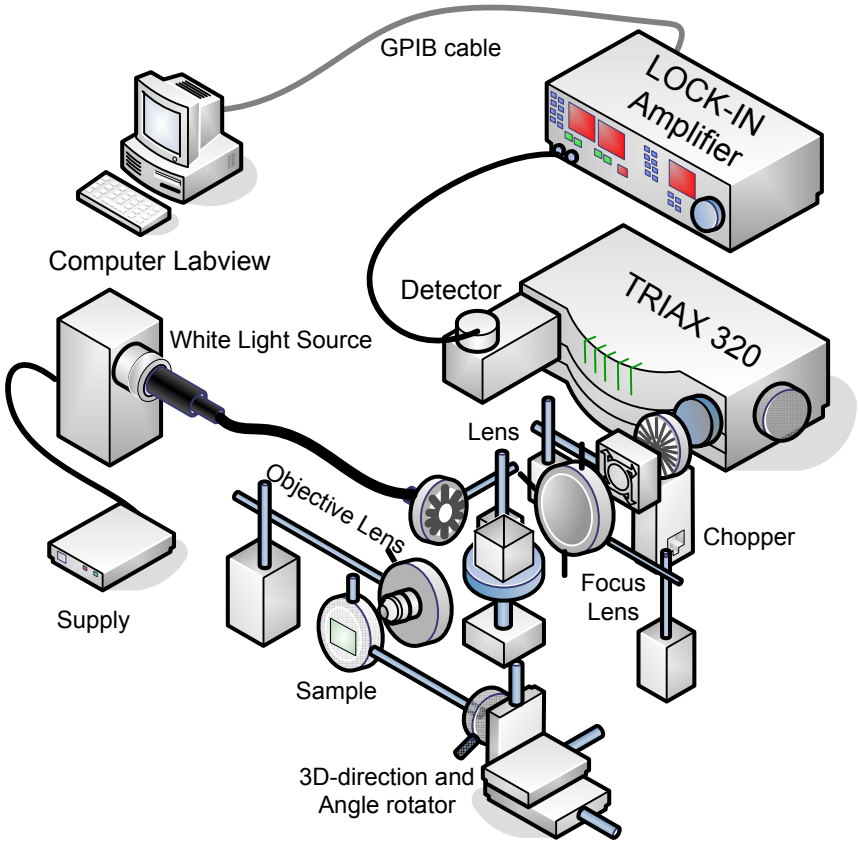

Figure 3.7 Schematic of reflection measurement for broadband reflectors.

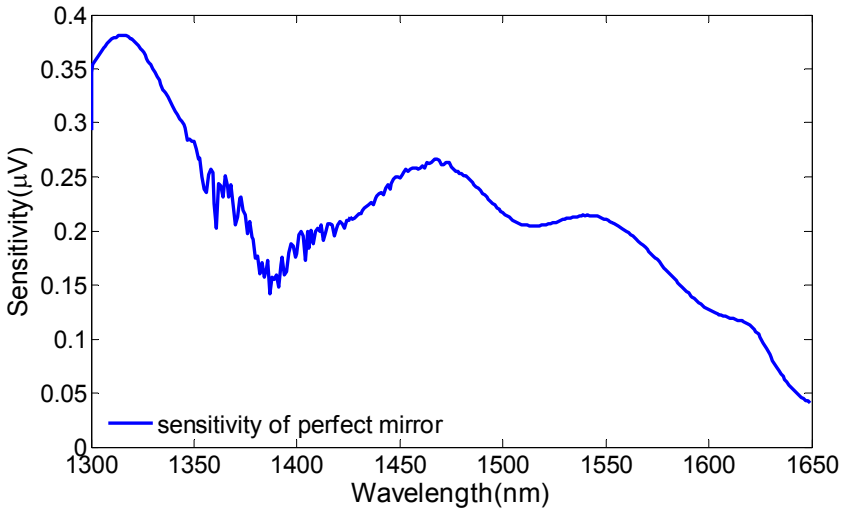

Figure 3.8 Reflection measurement of broadband metallic protected gold mirror.

For narrowband filters, the transmission spectra will be obtained to characterize the properties of these filters, and the design parameters such as lattice constant (a) and airhole radius (r) are focused on the region starting from 1300 nm to 1650 nm which is inside infrared region (IR) and dip location at wavelength operation of 1550 nm. The schematic of transmission measurement is demonstrated in Figure 3.9. From transmission setup, the device and the PET substrate used as a reference are mounted on the sample holder which can be moved freely in three-dimensional (3D) directions in order to control focused beam light on the patterned area, and can be changed incident angle (θ) which is the angle off surface normal, and rotation angle which is the angle ϕ with respect to ΓX, or polarization angle (Ψ) which is the angle with reference to the ΓM direction as shown in inset of Figure 3.10. First, pointing focused beam of light source which is broadband quartz tungsten halogen (QTH) on the PET substrate until obtaining maximum sensitivity at lock-in amplifier by adjusting the 3D sample holder. Then, the transmission spectra of the PET substrate will be measured by using labview. Second, when focused beam light gets through the iris diaphragm which is opened as a small spot then passes through controllable polarizer and objective lens, beam light spot will focus on a filter

and pass through a focal lens to focus light to the chopper get into the spectrometer. From there the light goes through the spectrometer slit which can be set to be narrow to reduce noises. Third, at the exit of the spectrometer, the signal is detected by the InGaAs IR detector. The signal detected by InGaAs IR detector will go to a lock-in amplifier. Consequently, the chopper frequency can be matched to that of the signal. Then it is rolled back to the labview program. After the data of PET substrate and filter were obtained, the reflection spectra of filter will be the data of filter normalized by those of PET substrate.

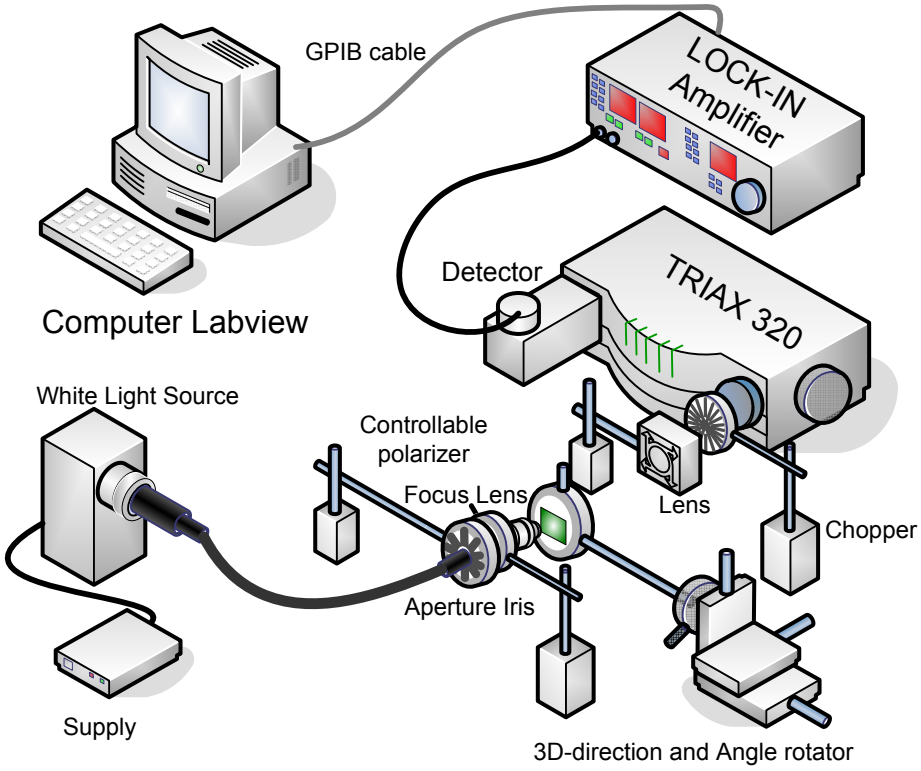

Figure 3.9 Schematic of transmission measurement for narrowband filters.

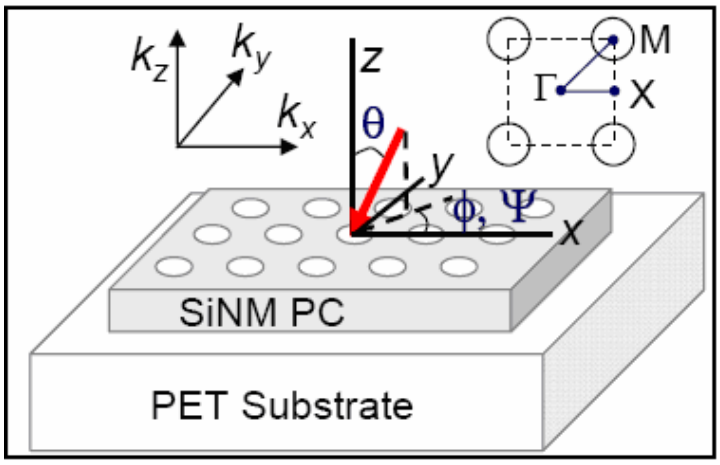

Figure 3.10 Schematic of measurement setup focusing on filter.[2]

3.3 SEM images

This section contains some SEM images of the broadband reflectors. The SEM images are divided into four categories which are composed of images of original devices, images of devices after BHF, images of devices after PECVD, and lastly, images of devices after spin coating with SOG.

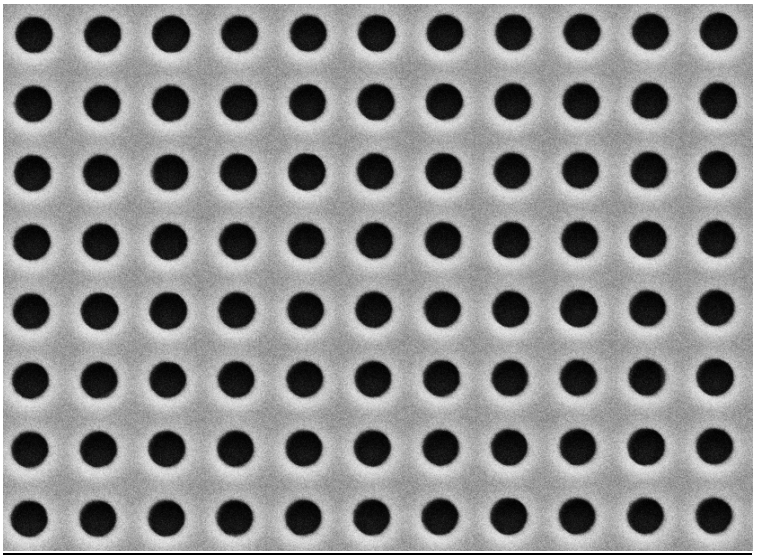

Figure 3.11 SEM images of broadband reflector without any SiO_2 on top of SiNMs.

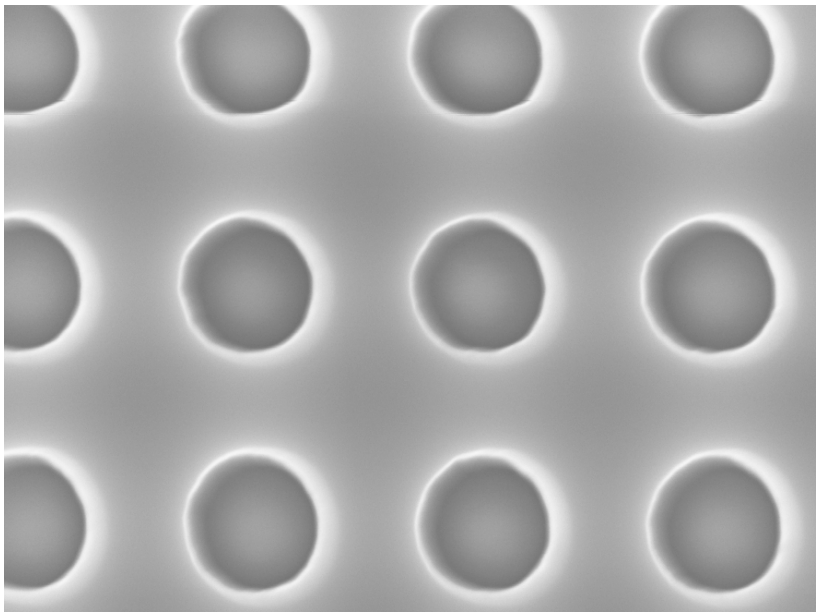

Figure 3.12 An SEM image of broadband reflector after BHF 3 minutes.

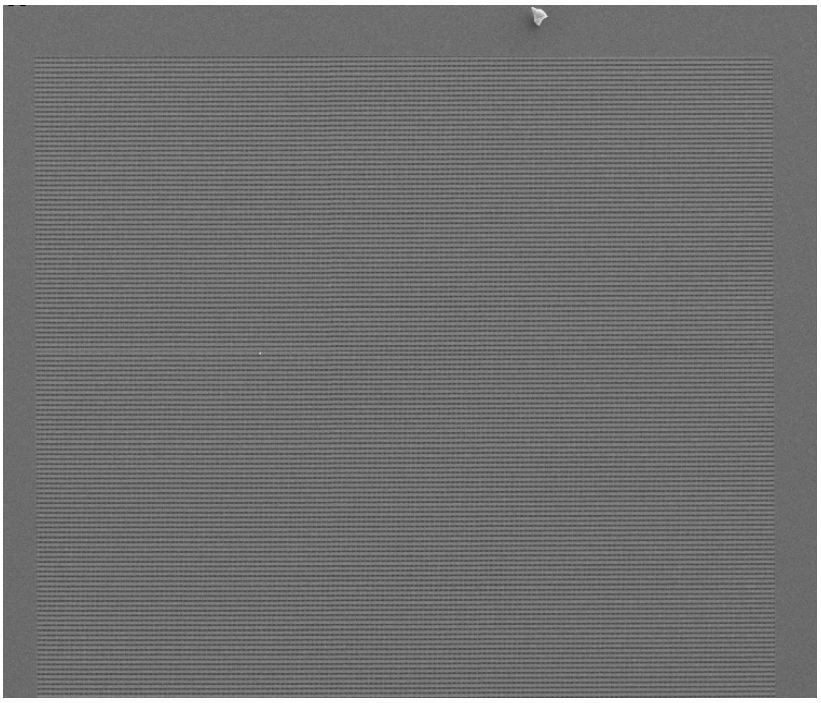

Figure 3.13 An SEM image of broadband reflector having area ~5x5 mm^2 after PECVD SiO_2 thickness 100 nm.

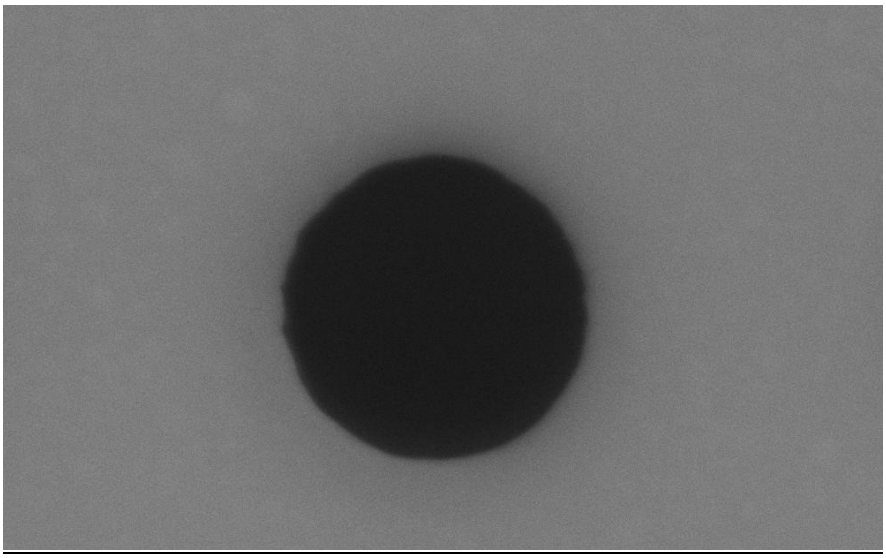

Figure 3.14 An SEM image of broadband reflector having lattice constant (a) 0.92μm and r/a 0.27 after PECVD SiO_2 thickness 100 nm.

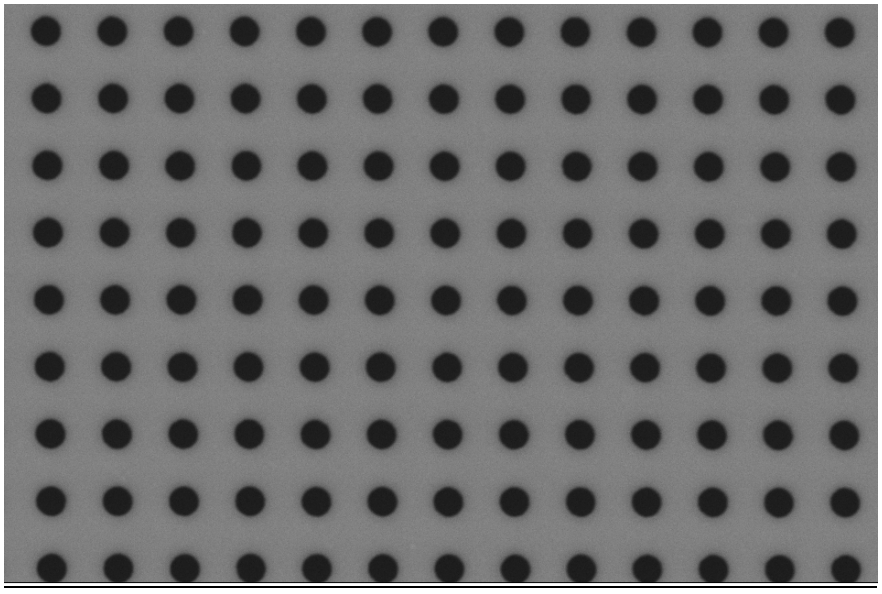

Figure 3.15 An SEM image of broadband reflector after PECVD SiO_2 thickness 200 nm.

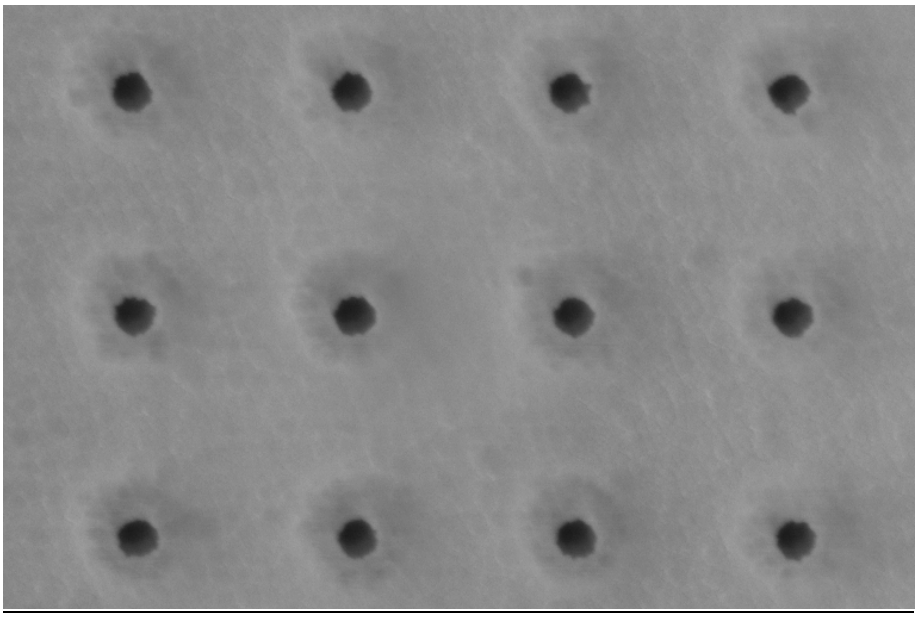

Figure 3.16 An SEM image of broadband reflector after PECVD SiO_2 thickness 500 nm.

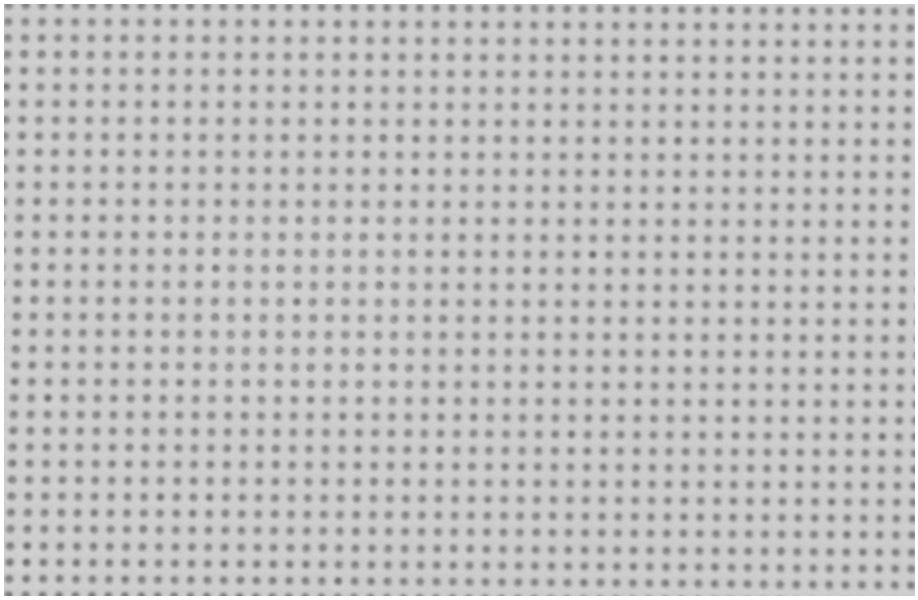

Figure 3.17 An SEM image of broadband reflector after SOG spin coating thickness 290 nm.

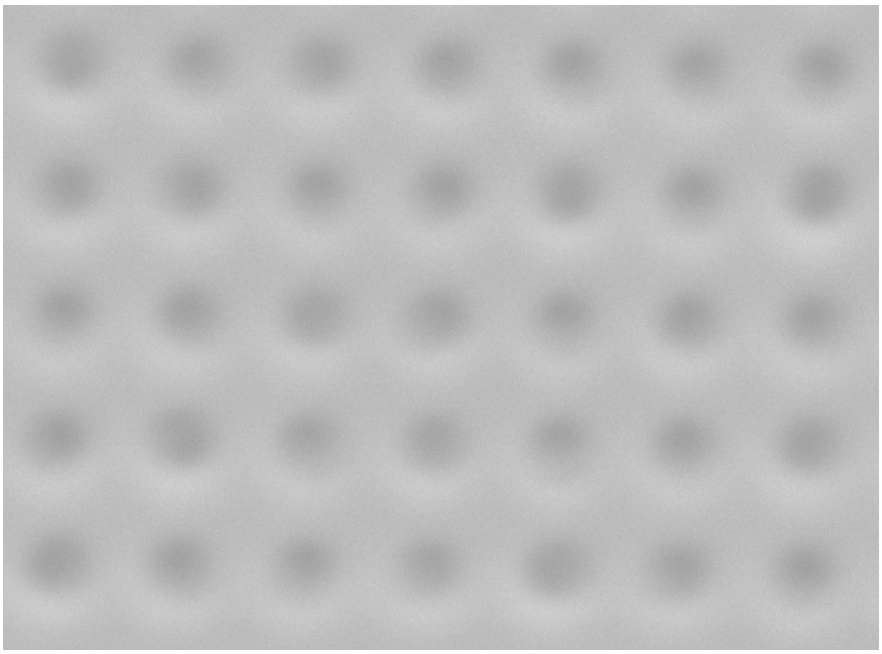

Figure 3.18 An SEM image of broadband reflector after spin coating with thickness 540.6 nm.

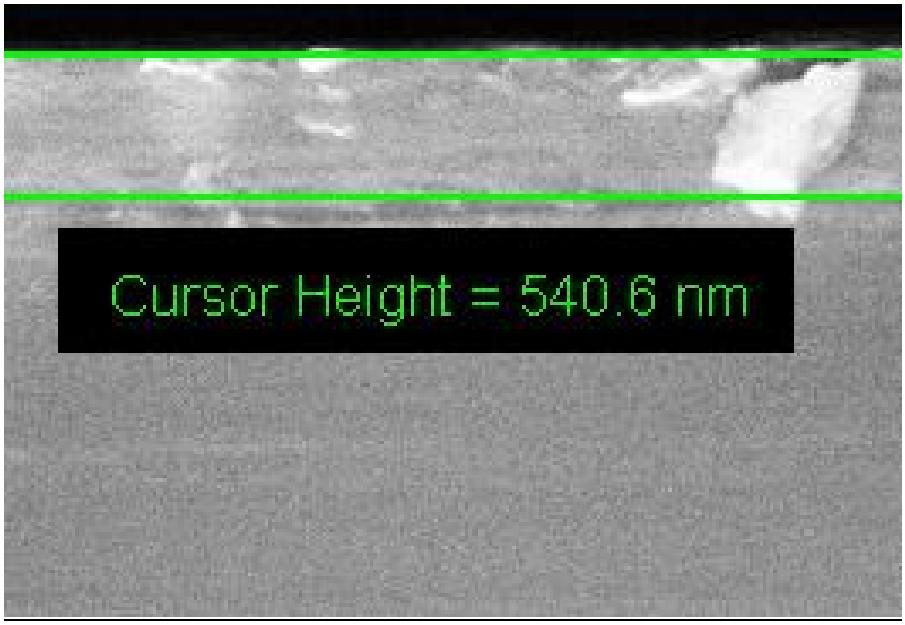

Figure 3.19 The thickness 540.6 nm after SOG spin coating.

3.4 Labview program

3.4.1 Labview instrument for tunable laser and OSA

All virtual instruments are developed in order to support transmission measurement for filters and I-V test for solar cell and VCSELs laser.

3.4.1.1 Serial port communication

In serial communication, the transmitter will send data to the receiver over a link line one bit at a time. Therefore, data can be sent at low transmission rate or over long distances by using this method. In addition, the serial port is the easy way to connect between two terminals since all computers have at least one serial port for common user's interface, so the additional installed hardware is not required.

RS-232 (Recommended Standard 232) is a standard for serial binary data interface between two terminals which are Data Terminal Equipment (DTE) and Data Communications Equipment (DCE) also including electrical signal characteristics such as voltage levels, and signal rates, connectors and pin identification, function of circuits in the interface connector etc.

3.4.1.2 The subVI to control tunable laser

In block diagram of labview, using the VIs located on Functions>>Instrument I/O>>Serial, there are VISA Configure Serial Port, VISA Write, VISA Read, and VISA Close that can be used for serial and GPIB port, therefore the tunable laser can be controlled for testing.

First, VISA Configure Serial Port VI initializes the serial port specified by VISA resource name to the specified settings. The details are as follows: Timeout sets the timeout value which default is 10000 milliseconds for the serial communication for the write and read operations. Baud rate is the transmission rate. Data bits is the number of incoming data bits. Stop bits serve as the last part of the frame. Parity which specifies parity for every frame to be transmitted or received, and flow control specify those specific serial port parameters. The error-in and error-out clusters maintain the error conditions for VI.

Second, VISA Write used to write the data from write buffer to the device or interface identified by VISA resource name. Vice versa, VISA Read used to read number of data in bytes from the device or interface into read buffer.

Finally, VISA Close will close the device which is identified by VISA resource name.

How it works. When the tunable laser switch at front panel is turned on, the true case structure at block diagram will be executed as shown in Figure 3.20 The VISA Write function will writes the write buffer string which contains all input data to the tunable laser specified by VISA resource name. Hence, input data which are WFR=1 and ENS=1 will be selected to turn on laser as shown in Figure 3.21. On the other hand, when the tunable laser switch at front panel is turned off, the false case structure at block diagram will be executed as shown in Figure 3.22 The VISA Write function will writes the write buffer string which contains all input data to the tunable laser specified by VISA resource name. Consequently, input data which are WFR=1 and ENS=0 will be selected to turn off laser.

In front panel of labview, this panel is used to change any input data like the users interface. In order to control tunable laser, the input data WFR=1 which is waiting for ready and ENS=1 which is enable laser used to turn on the tunable laser, on the other hand, the input data WFR=1 and ENS=0 which is disable laser used to turn off the tunable laser. In addition to input data to turn on and off laser, the input data PW1 is employed to get the laser power for each channel from ch1 to ch200 ,and clear fault flags can be achieved by using CFF=hhh.

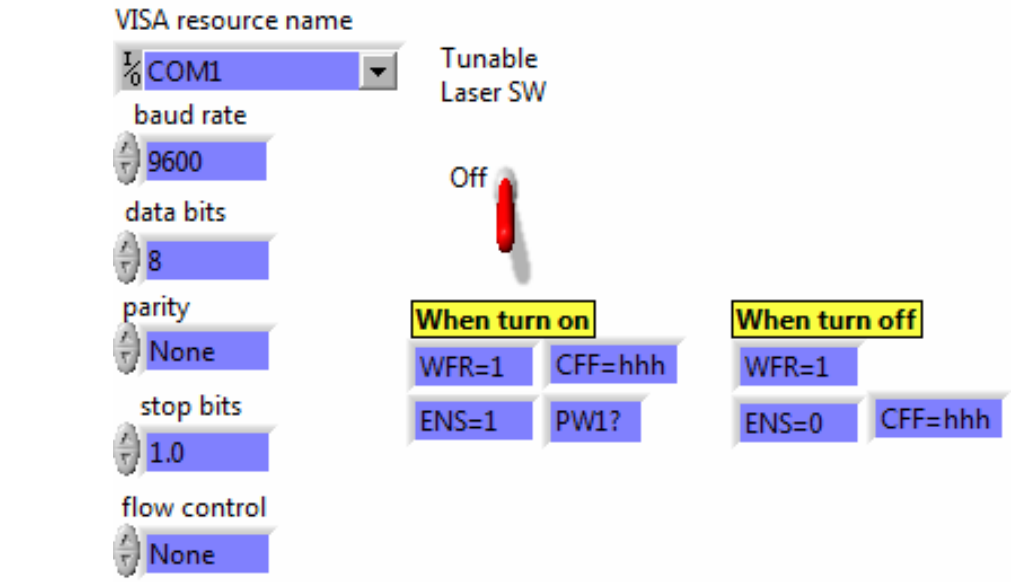

Figure 3.20 Front panel to enable tunable laser.

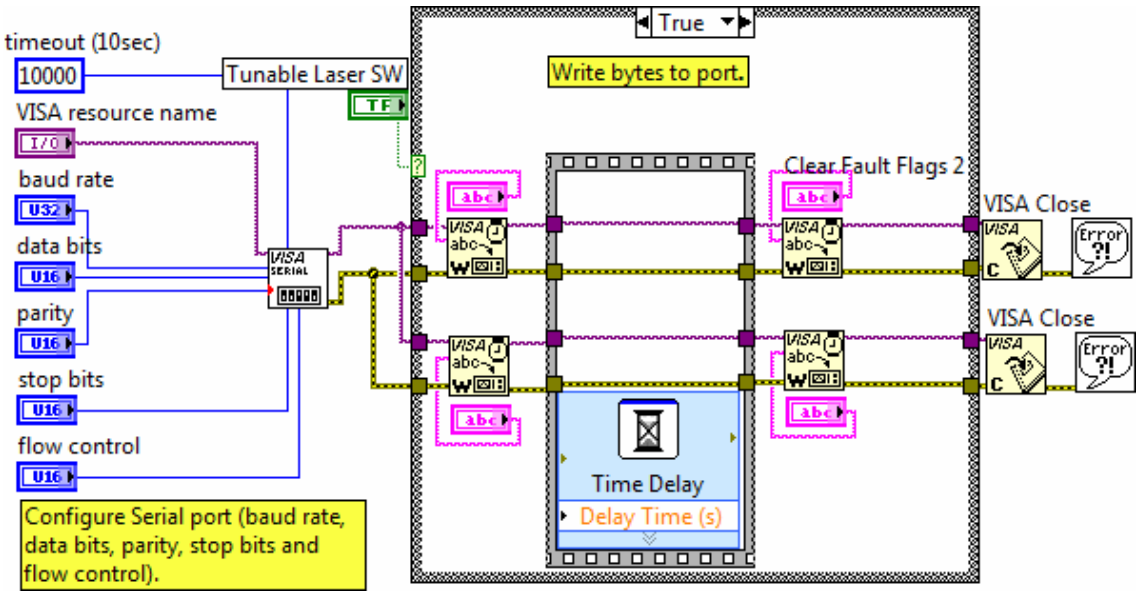

Figure 3.21 Block diagram to enable tunable laser when case structure is true.

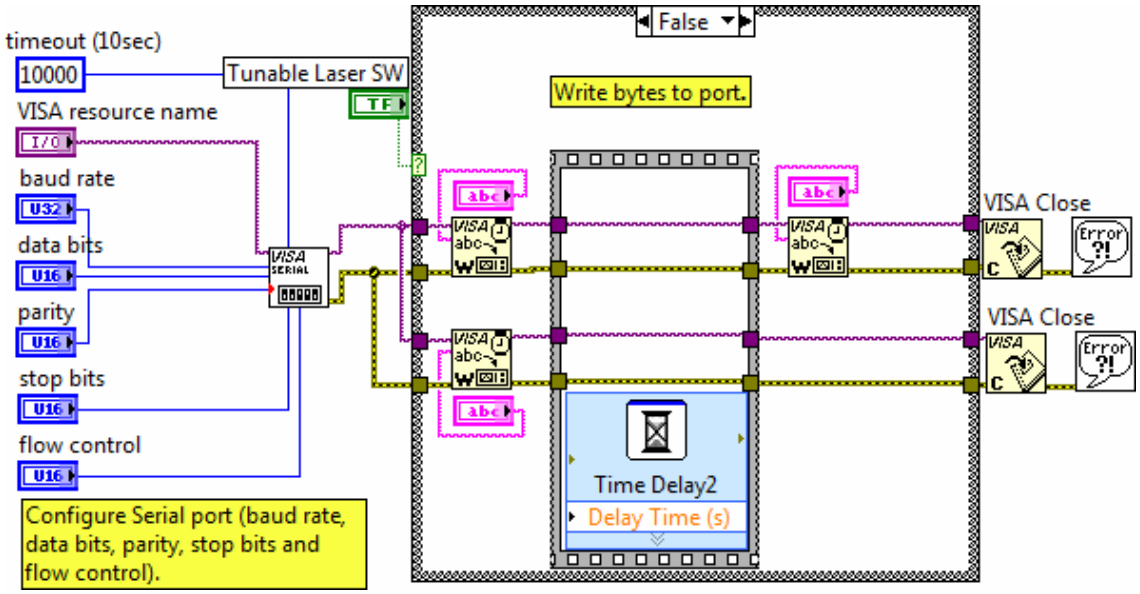

Figure 3.22 Block diagram to disable tunable laser when case structure is false.

In order to get output power each channel of tunable laser, in block diagram , based on the tunable laser specifications, channel 1 starts from wavelength 1527.4 nm at frequency 196.275 THz and the adjacent channel which is channel 2 having the increment about 0.2 nm will be at 1527.6 nm at frequency 196.250 THz until the last channel which is channel 200 has peak at wavelength 1567.1 nm at frequency 191.300 THz. these information can be plugged into the loop_laser subVI as shown in Figure 3.23 which is a subVI that users can input channel number, and output will be the laser power, wavelength, and frequency for each channel. In loop_laser subVI, another subVI which is channel_power subVI has time delay that put between case structure write and read so as to make tunable laser and labview program synchronous.

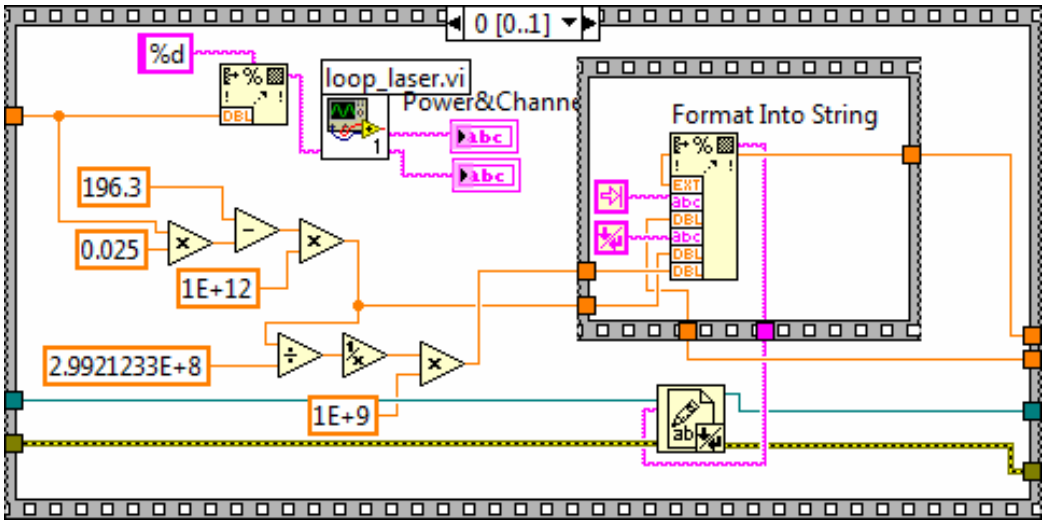

Figure 3.23 Block diagram connecting to loop_laser subVI to input ch# and get laser power.

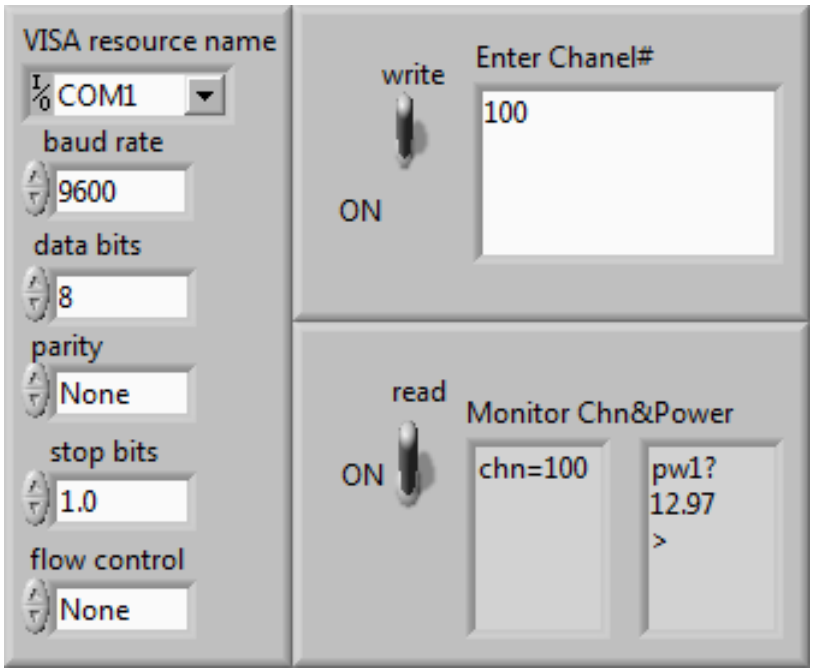

Figure 3.24 Front panel of channel_power subVI to write input and read output data.

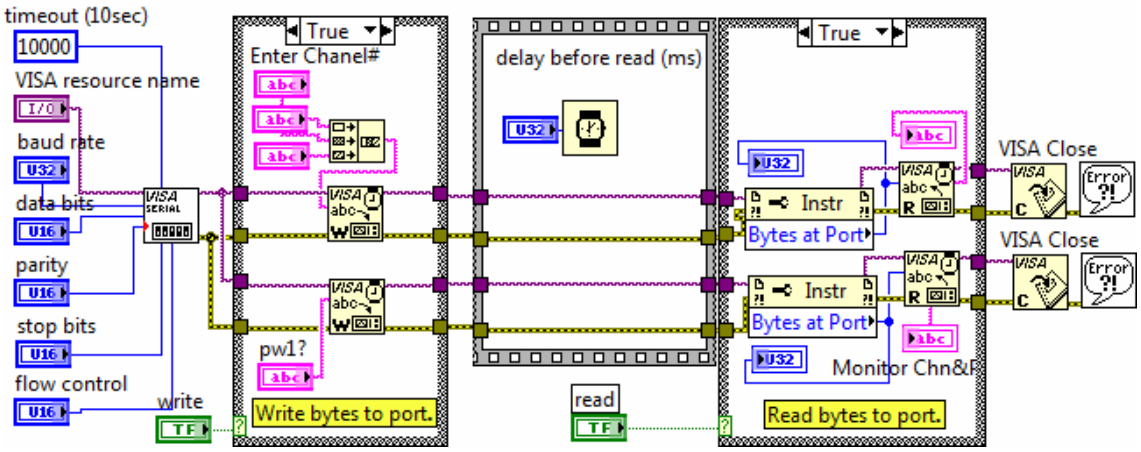

Figure 3.25 Block diagram of channel_power subVI when case structure is true.

How it works. All input data in a channel_power subVI will be transferred from a loop_laser subVI. In block diagram of channel_power subVI, when both switches at front panel is turned on as shown in Figure 3.24, the left true case structure in this block diagram will be executed as shown in Figure 3.25. The VISA Write function will writes the write buffer string which contains all input data to the tunable laser specified by VISA resource name. Hence, input data which are channel number and laser power will be selected. Another true case structure on the right-hand side in this block diagram will also be executed as shown in Figure 3.25. The VISA Read function will read the input data specified by VISA resource name and returns the data into read buffer. Hence, the output data will show the channel number and laser power at that channel as show in Figure 3.24 at read windows.

On the other hand, when both switches at front panel is turned off as shown in Figure 3.26, the both false case structures in this block diagram will be executed as shown in Figure 3.27. Consequently, this process can be used to check tunable laser that can interact with labview well or not.

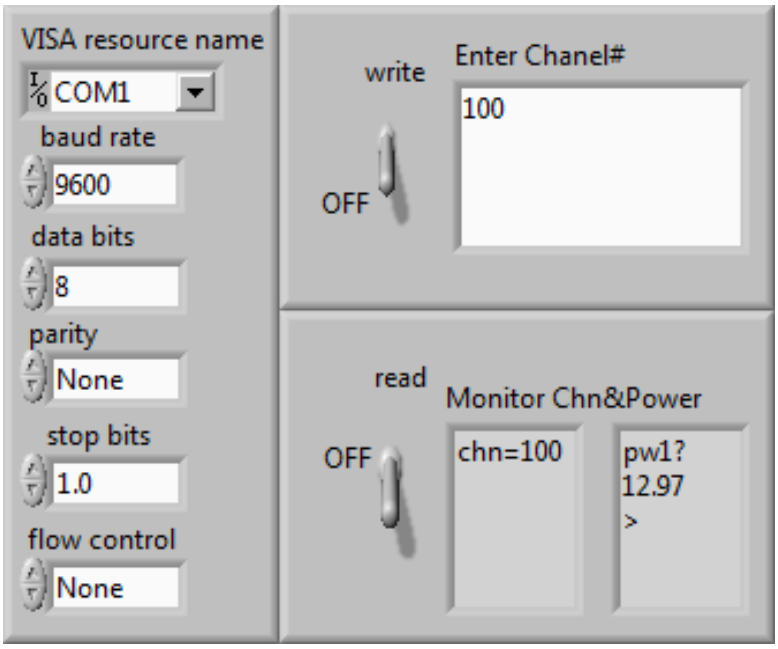

Figure 3.26 Front panel of channel_power subVI when both switches turn off.

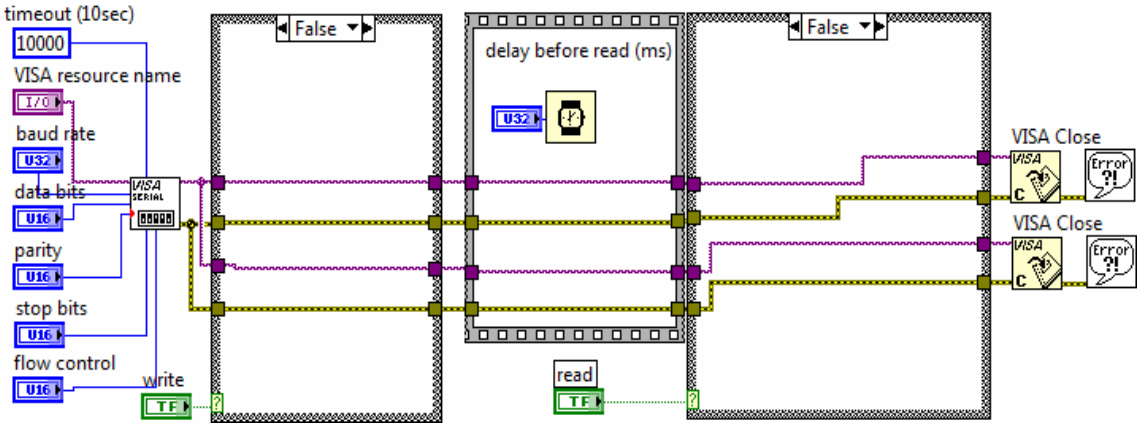

Figure 3.27 Block diagram of channel_power subVI when case structure is false.

3.4.1.3 The subVI to control optical spectrum analyzer

In Front panel, From optical spectrum analyzer (OSA) VI, Tunable laser can be sweep continuously from the first to the last channel, or can be sweep with specific increment from any channel to last desired one as shown in Figure 3.28, for example, sweeping tunable laser from channel 5 to channel 100 with increment 5, so in this case, the first one will be channel 5 and the second will be 10 and so on. The input data will be entered into a loop_laser subVI which provided the channel number, laser power, wavelength, and frequency. For interface, GPIB (General Purpose Interface Bus) can be used to communicate between labview and OSA. In block diagram of labview, using the VIs located on Functions>>Instrument I/O>>GPIB, there are GPIB Read, GPIB Write that can be used for GPIB interface bus, as a result, the OSA can be controlled for testing. Data that can be write to or read from OSA are provided by product company. In manual of OSA, such data are commonly called programming commands[10] which are shown in Figure 3.29. The OSA VI can be clearly explain step by step as follows.

First, GPIB Write is used to write data to OSA identified by GPIB address, and GPIB address can be set, and in our case, it equals to 13 as shown in Figure 3.28. Simultaneously, at block diagram, the command SNGLS which means “select single sweep mode” also is written to the OSA which is the device to be controlled as shown in Figure 3.30. Then, the command CEN TERWL which means “center wavelength” will be written to the OSA. After that, GPIB Read will read center wavelength data from the OSA and send it to sequence local for showing output data and keep it for saving data by concatenate strings subVI as shown in Figure 3.31.

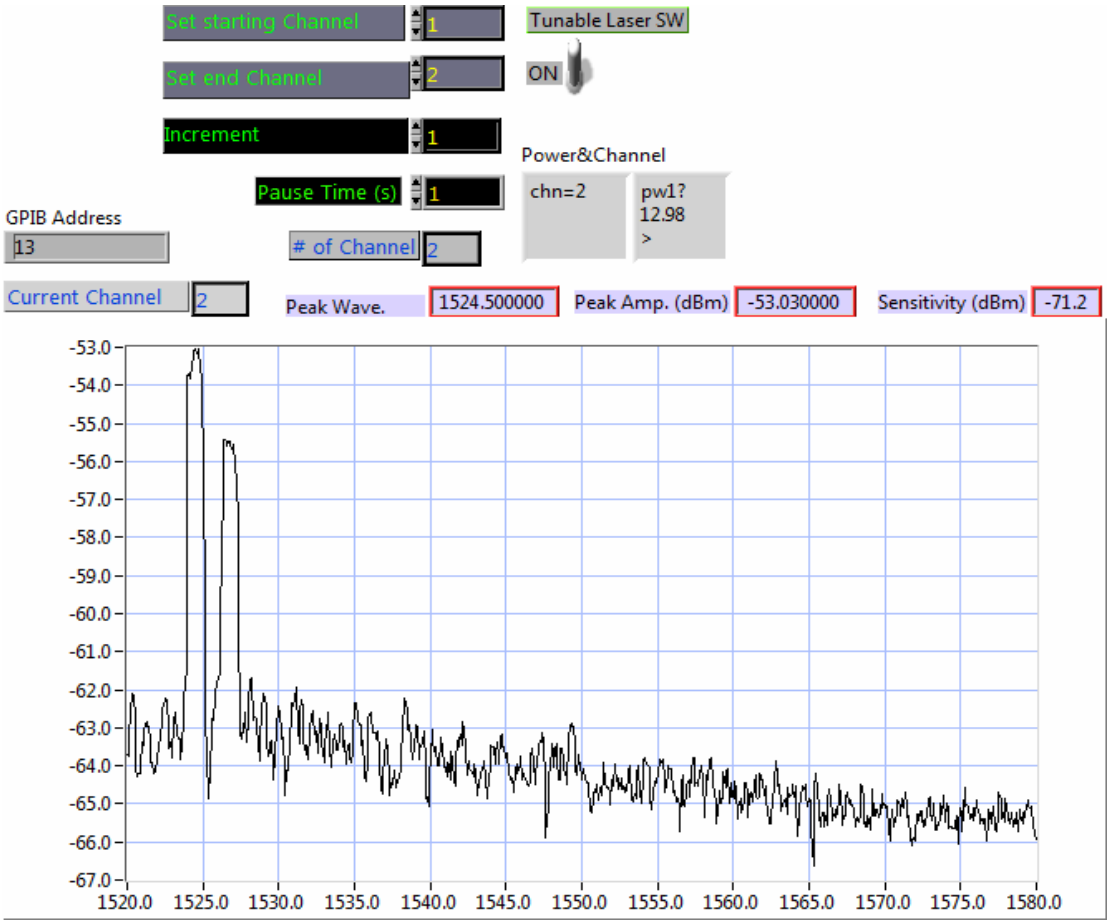

Figure 3.28 Front panel of OSA VI.

Programming Commands for OSA VI
TRA : Trace Data Input and Output
SNGLS : Selects single sweep mode.
CONTS : Continuous Sweep
SENS : Selects the input sensitivity level.
STOPWL : Sets the stop wavelength. Related command
STARTWL : Start wavelength
CENTERWL:Center Wavelength
MKPK : Position active marker at a peak (or pit) on the trace.
MKA : Specifies the amplitude of the active marker.
MKWL : Position active marker to the specified wavelength, or return the marker wavelength.
SP : Sets the wavelength span. Related command:
RB : Sets the resolution bandwidth.

Figure 3.29 All of the programming commands for OSA.

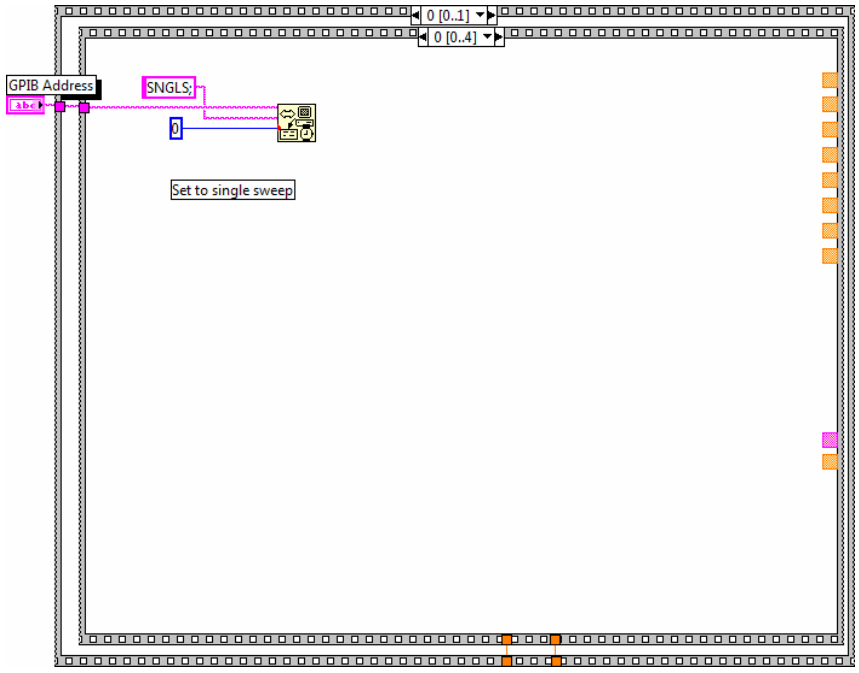

Figure 3.30 Block diagram of OSA VI employed to write command SNGLS to OSA.

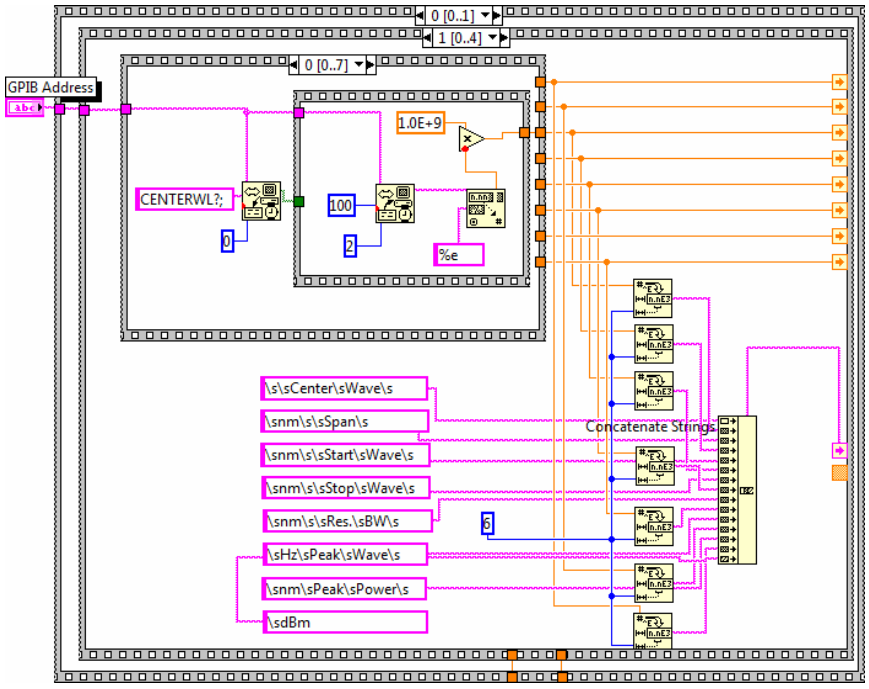

Figure 3.31 Block diagram of OSA VI employed to write command CENTERWL to OSA.

Second, every process is similar to the first step except changing command from CENTERWL to SP as shown in Figure 3.32. Then, the command SP which means “set the wavelength span” will be written to the OSA. After that, GPIB Read will read wavelength span data from the OSA and send it to another sequence local for showing output data and keep it for saving data by the same concatenate strings subVI as shown in Figure 3.32.

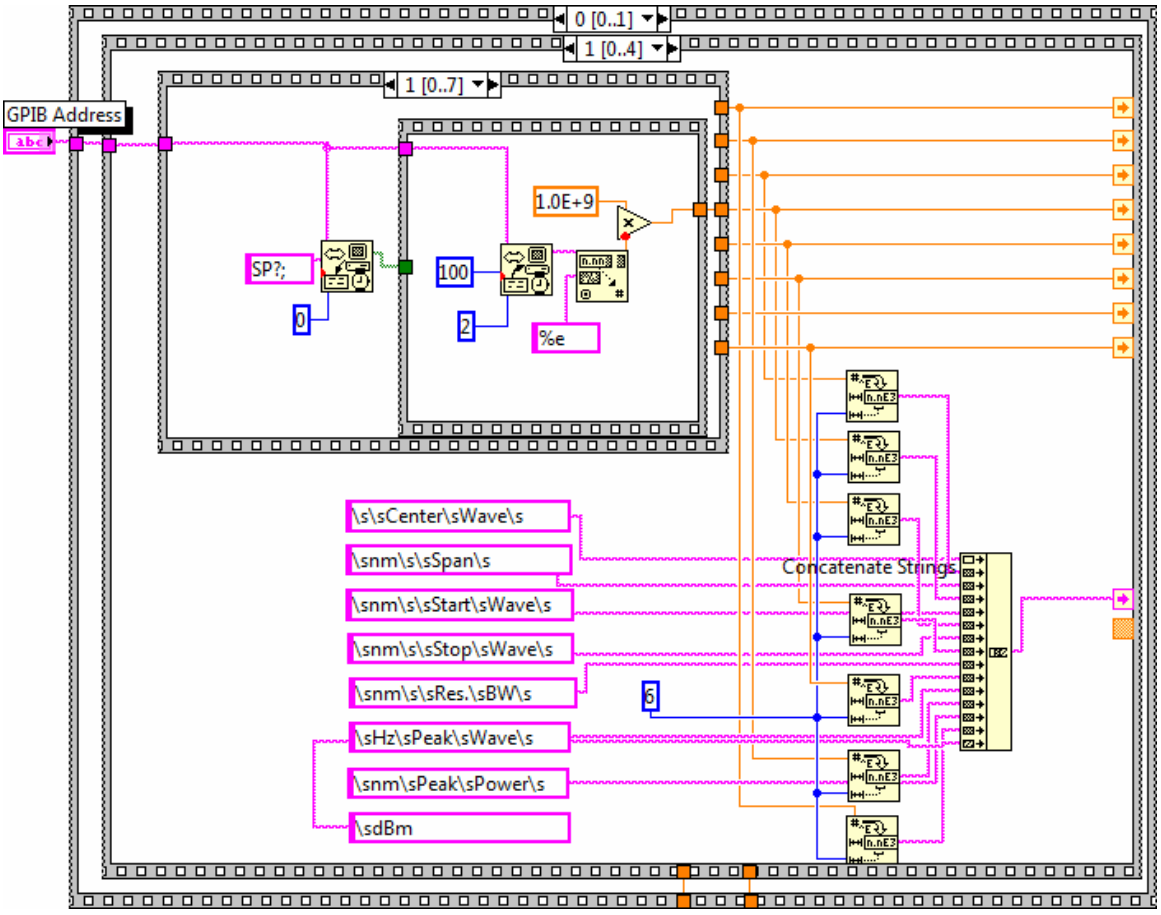

Figure 3.32 Block diagram of OSA VI employed to write command SP to OSA.

Third, every process is the same as the second step except changing command from SP to STARTWL as shown in Figure 3.33. Then, the command STARTWL which means “set start wavelength” will be written to the OSA. After that, GPIB Read will read start wavelength data from the OSA and send it to another sequence local for showing output data and keep it for saving data by the same concatenate strings subVI as shown in Figure 3.33.

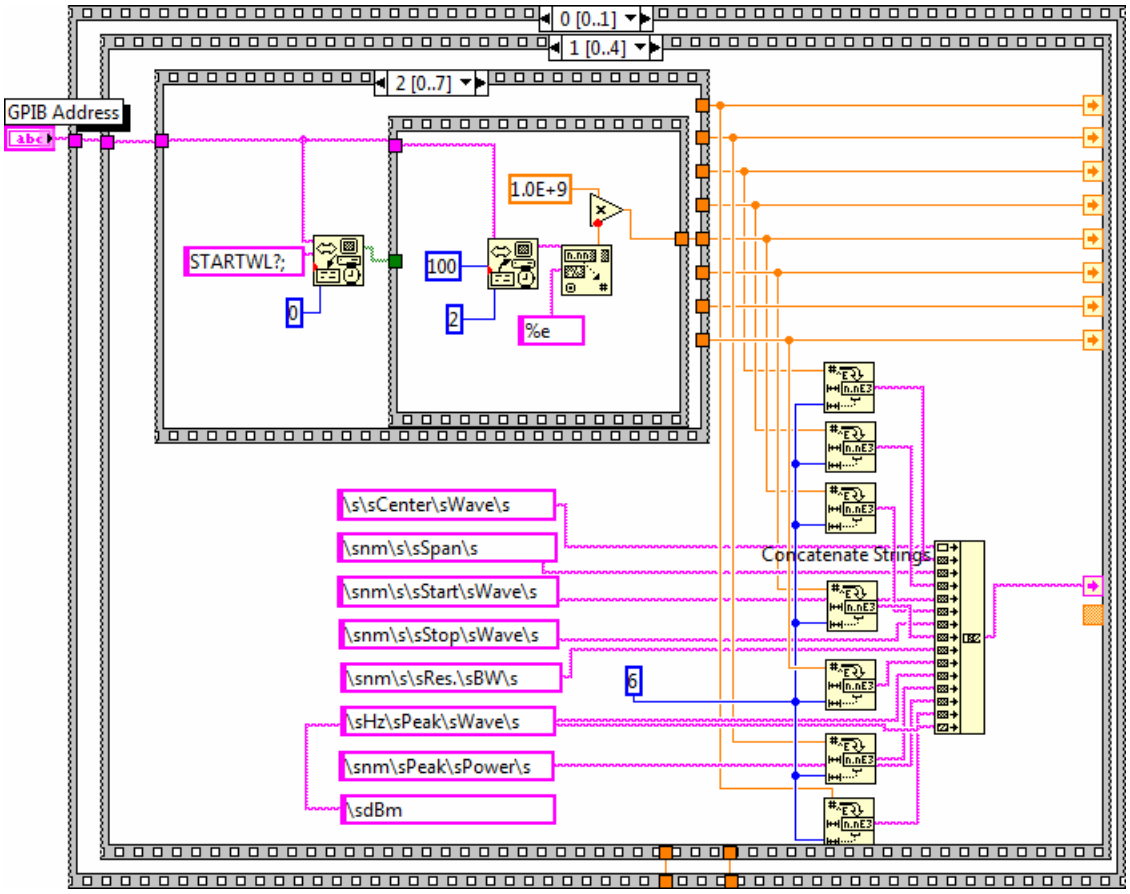

Figure 3.33 Block diagram of OSA VI employed to write command STARTWL to OSA.

Fourth, every process is the same as the third step except changing command from STARTWL to STOPWL as shown in Figure 3.34. Then, the command STOPWL which means “set stop wavelength” will be written to the OSA. After that, GPIB Read will read stop wavelength data from the OSA and send it to another sequence local for showing output data and keep it for saving data by the same concatenate strings subVI as shown in Figure 3.34.

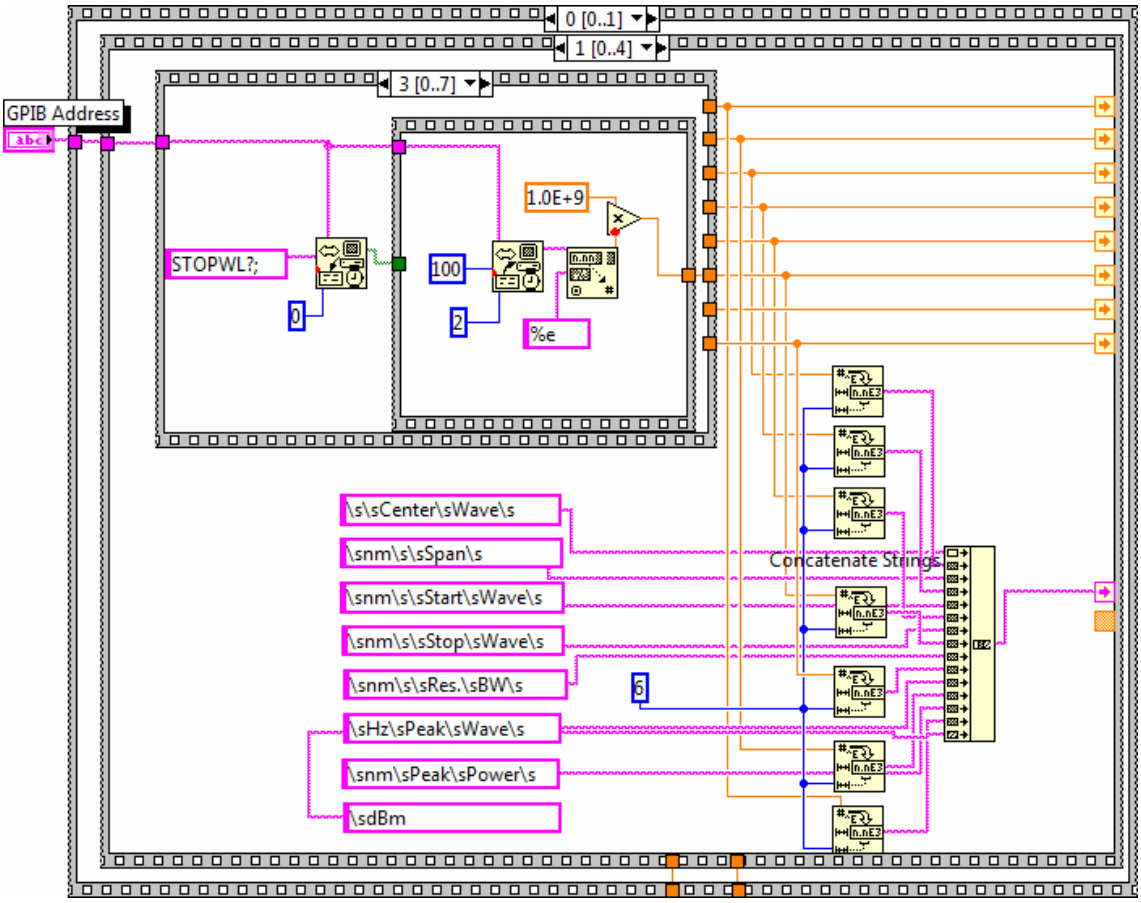

Figure 3.34 Block diagram of OSA VI employed to write command STOPWL to OSA.

Fifth, every process is the same as the fourth step except changing command from STOPWL to SENS as shown in Figure 3.35. Then, the command SENS which means “select the input sensitivity level” will be written to the OSA. After that, GPIB Read will read input sensitivity level data from the OSA and send it to another sequence local for showing output data and keep it for saving data by the same concatenate strings subVI as shown in Figure 3.35.

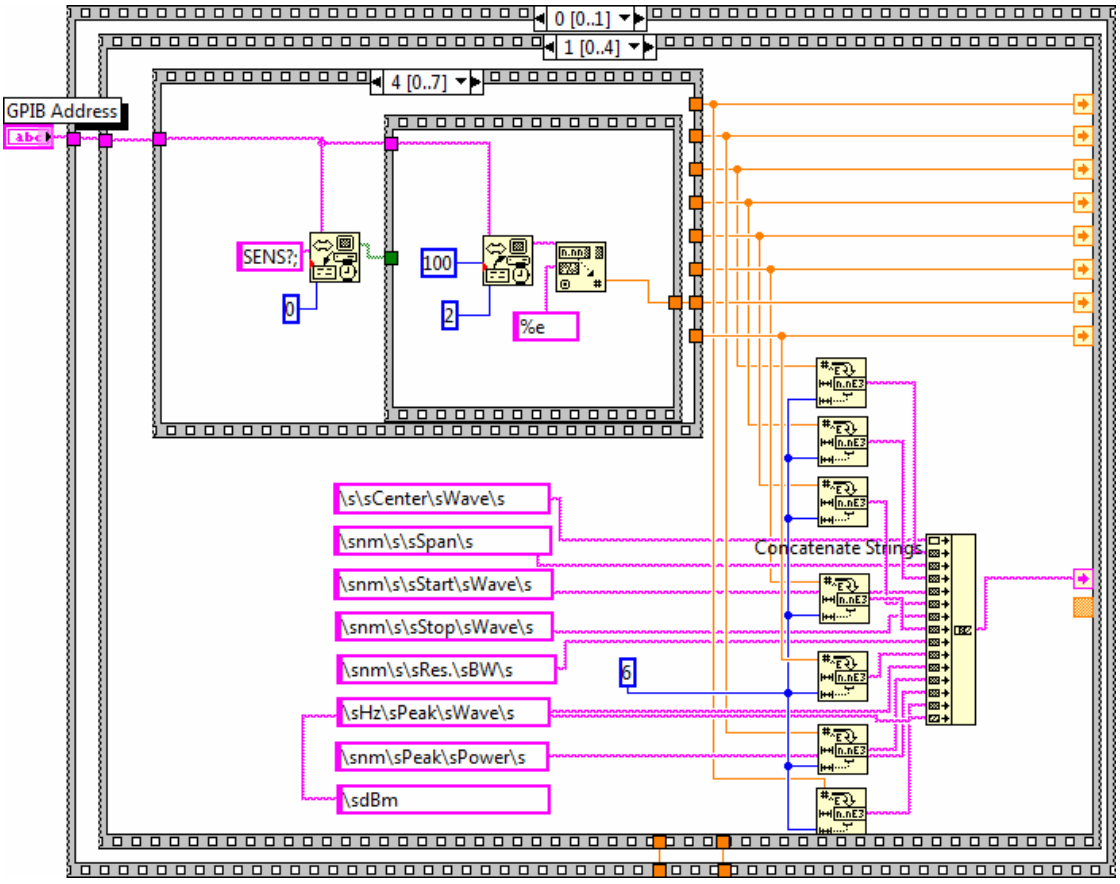

Figure 3.35 Block diagram of OSA VI employed to write command SENS to OSA.

Sixth, every process is the same as the fifth step except changing command from SENS to RB as shown in Figure 3.36. Then, the command RB which means “set the resolution bandwidth” will be written to the OSA. After that, GPIB Read will read the resolution bandwidth data from the OSA and send it to another sequence local for showing output data and keep it for saving data by the same concatenate strings subVI as shown in Figure 3.36.

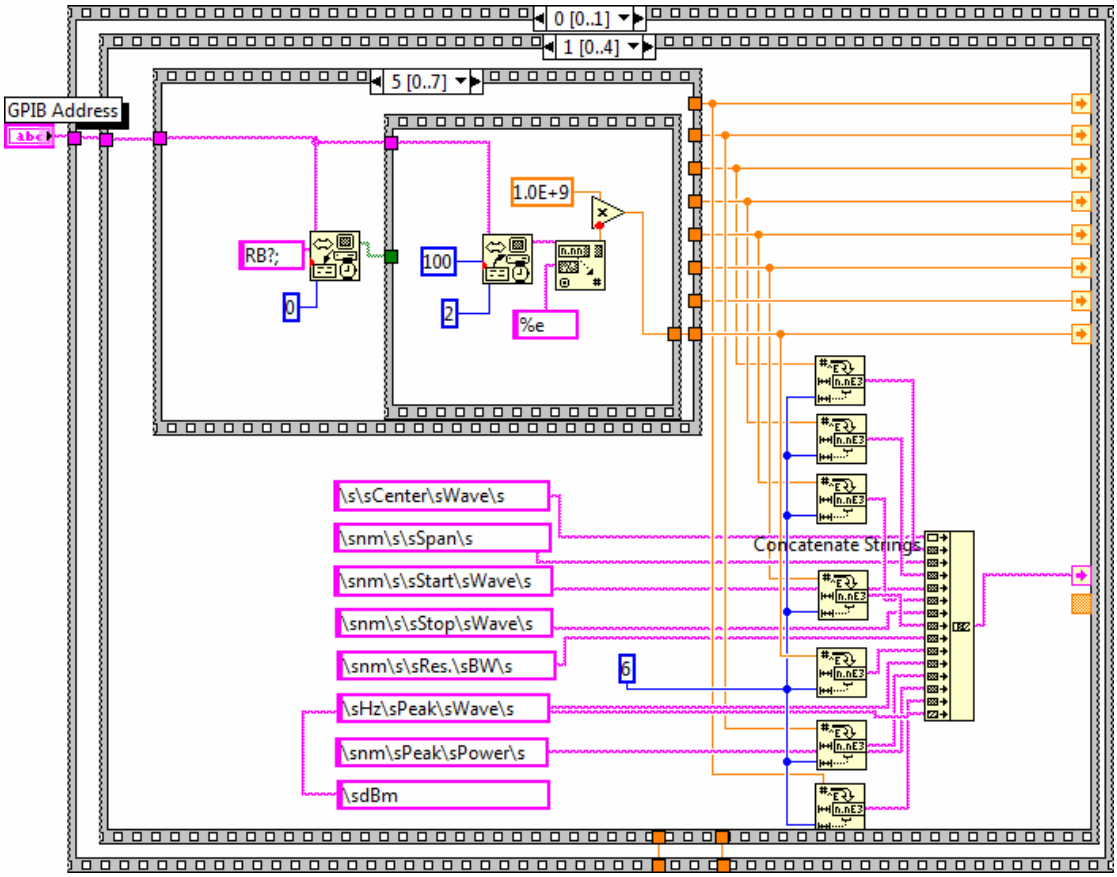

Figure 3.36 Block diagram of OSA VI employed to write command RB to OSA.

Seventh, every process is the same as the sixth step except changing command from RB to MKPK and MKWL as shown in Figure 3.37. Then, the command MKPK and MKWL which means “set mark peak and marker wavelength” will be written to the OSA. After that, GPIB Read will read maker peak and marker wavelength from the OSA and send it to another sequence local for showing output data and keep it for saving data by the same concatenate strings subVI as shown in Figure 3.37.

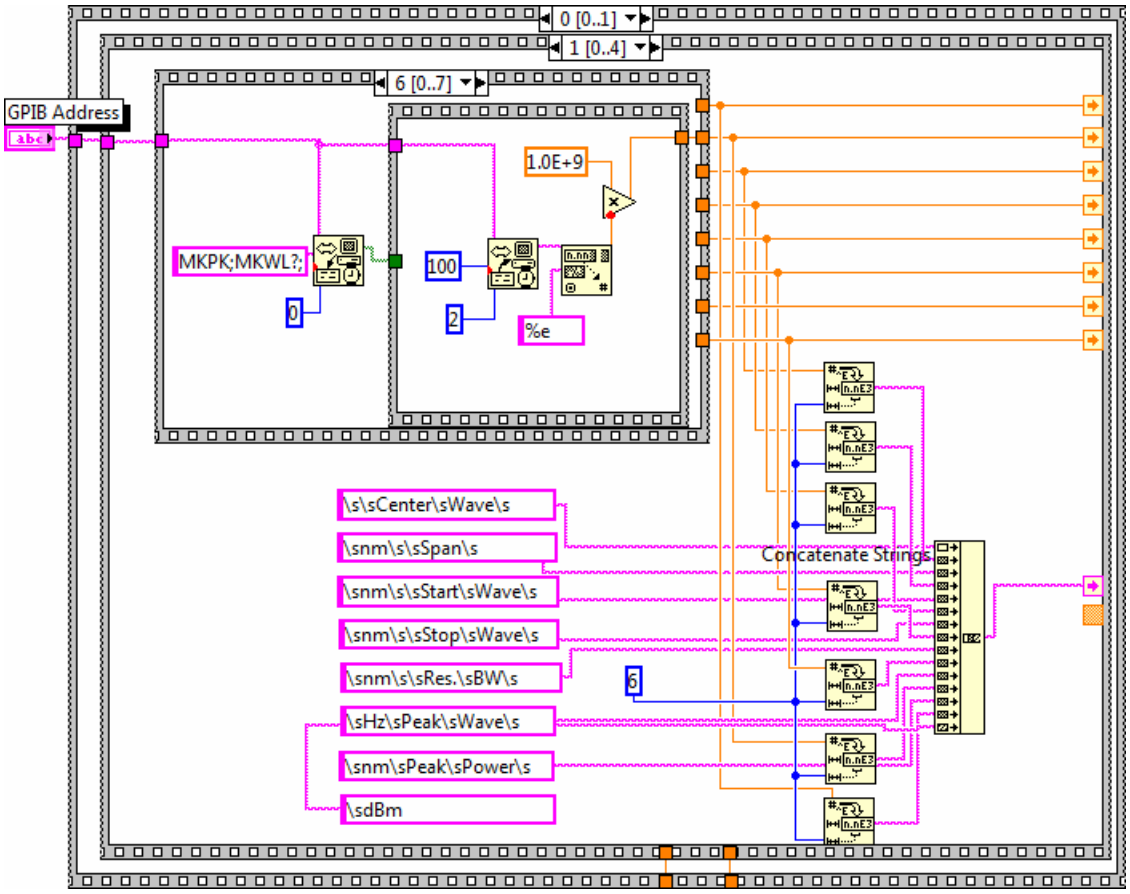

Figure 3.37 Block diagram of OSA VI employed to write command MKPK and MKWL to OSA.

Eighth, every process is the same as the seventh step except changing command from MKPK and MKWL to MKA as shown in Figure 3.38. Then, the command MKA which means “marker amplitude” will be written to the OSA. After that, GPIB Read will read marker amplitude data from the OSA and send it to another sequence local for showing output data and keep it for saving data by the same concatenate strings subVI as shown in Figure 3.38.

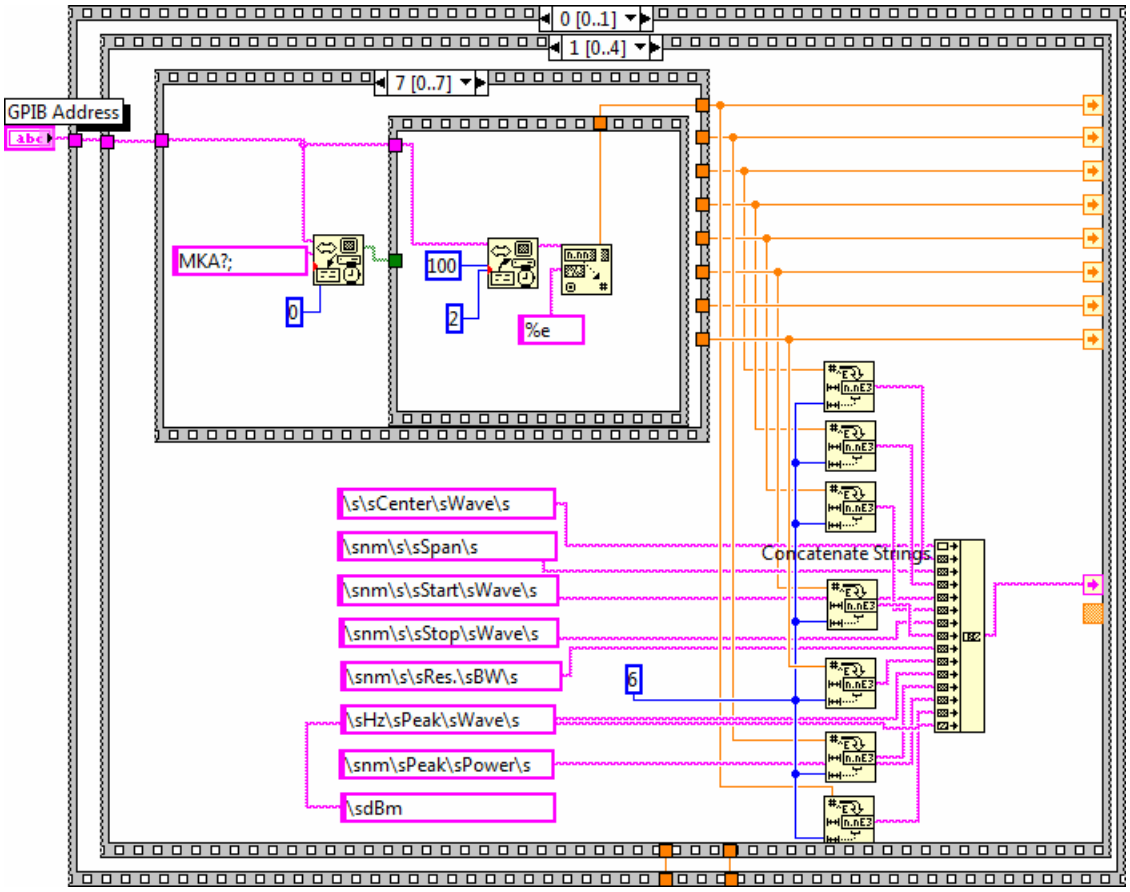

Figure 3.38 Block diagram of OSA VI employed to write command MKA to OSA.

Ninth, , GPIB Write is used to write data to OSA identified by GPIB address, and GPIB address can be set, and in our case, it equals to 13 as shown in Figure 3.39. Then, the command TRA which means “trace data input and output” will be written to the OSA. After that, output data form all sequence locals from step 1 to 8 that mentioned before will show at the front as shown in Figure 3.39.

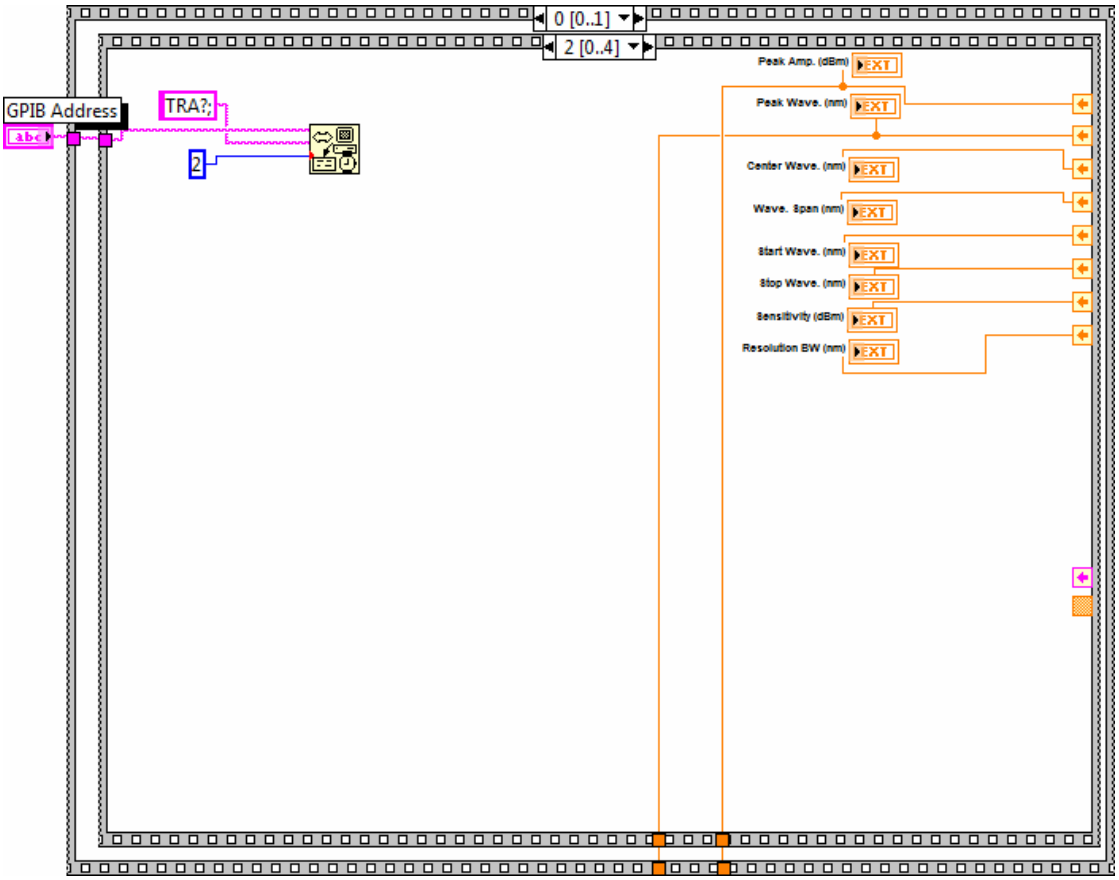

Figure 3.39 Block diagram of OSA VI employed to write command MKPK and MKWL to OSA.

Tenth, GPIB Read is used to read data from OSA identified by GPIB address. Then, the subtraction of output data “stop wavelength” and “start wavelength” will be divided into 800 steps which are used for For Loop to plot the peak spectra at each wavelength between start wavelength and stop wavelength as shown in Figure 3.40.

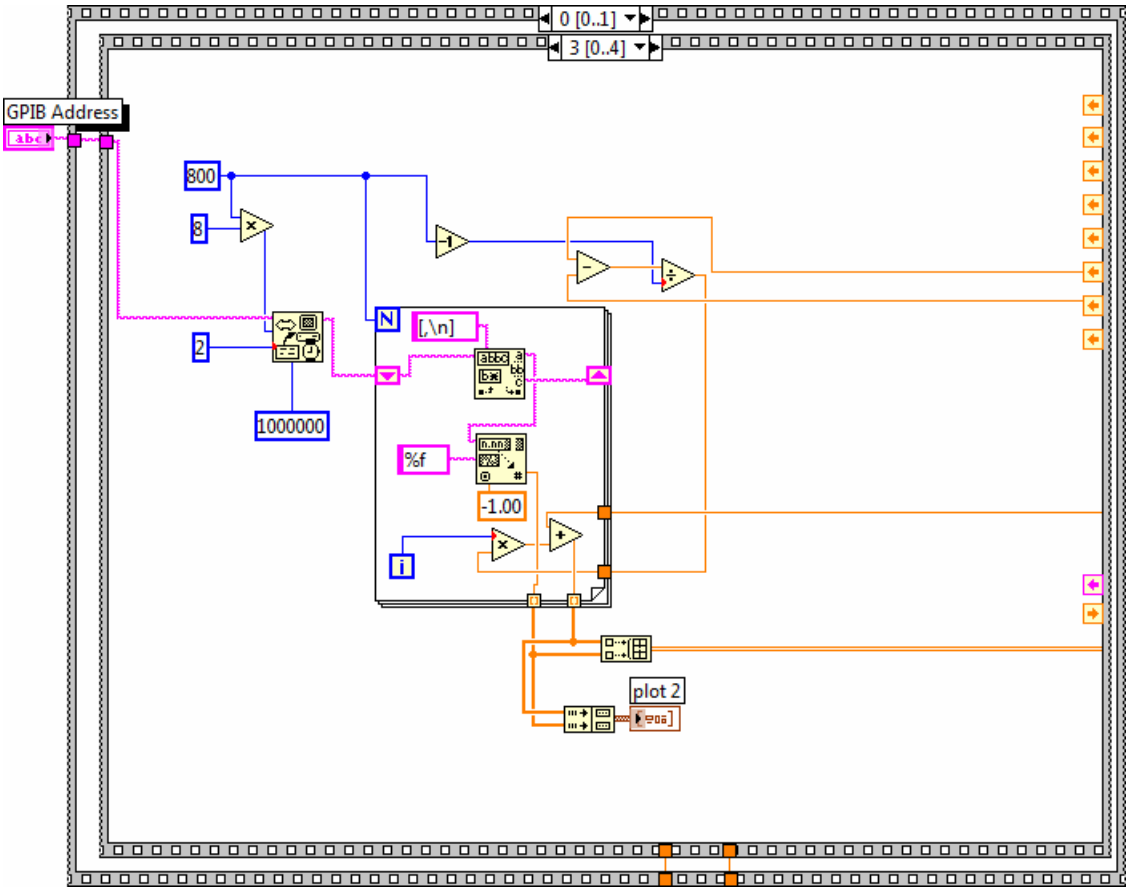

Figure 3.40 Block diagram of OSA VI used to plot peak spectra from start to stop wavelength.

Finally, it is true or false case structure that used to save or not save respectively all out put data into text file as shown in Figure 3.41.

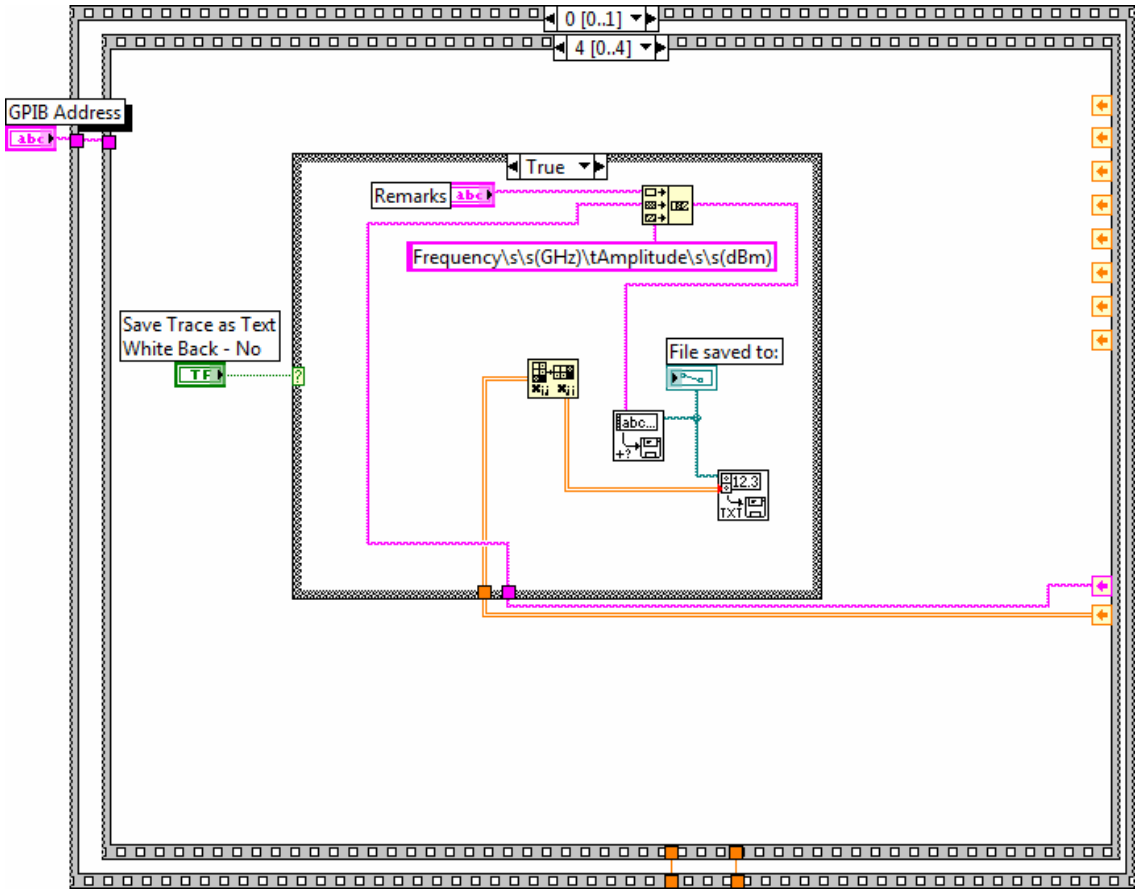

Figure 3.41 Block diagram of OSA VI used to save all output data into text file.

The reflection spectra of narrowband filter after measured by Photoluminescence (PL) test, and tunable Laser (T) test shown in Figure 3.42. From Figure, we summarize the points as follows:

1. Reflection spectra obtained by tunable laser test can be measured lower comparing to PL test, but the dip is not sharp.

2. The dip location almost the same point for both tests.

3. In tunable laser test, the OSA probably not stable, especially at dip location.

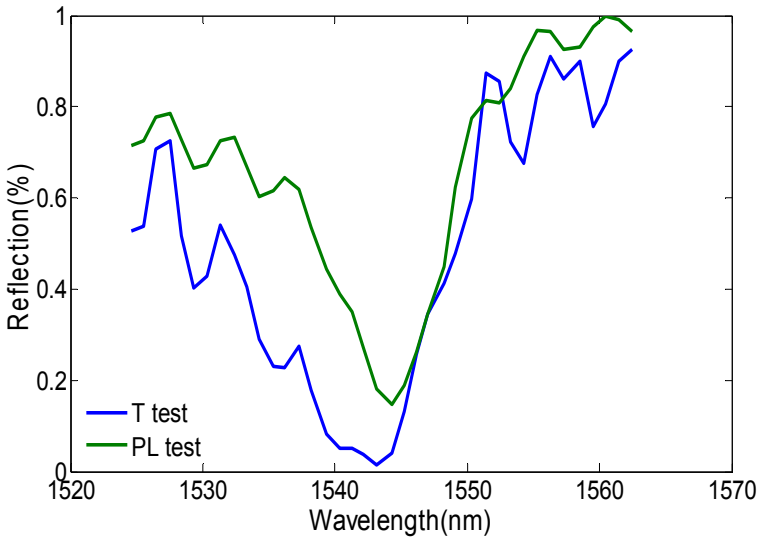

Figure 3.42 Reflection spectra comparing between PL test and tunable laser test.

The schematic of tunable laser test for narrowband filters is shown in Figure 3.43. From that Figure, tunable laser used as a light source can operate at different wavelengths starting from channel1 at 1527.6 nm to channel200 at 1567.1 nm. Focusing the light source on the filters and adjusting the sample location until getting the maximum output power at the OSA. Then, we measure the reflection spectra of filter and reference which is polyethylene terephthalate (PET) using labview program. Reflection spectra of filters are normalized by data of reference material shown in Figure 3.42.

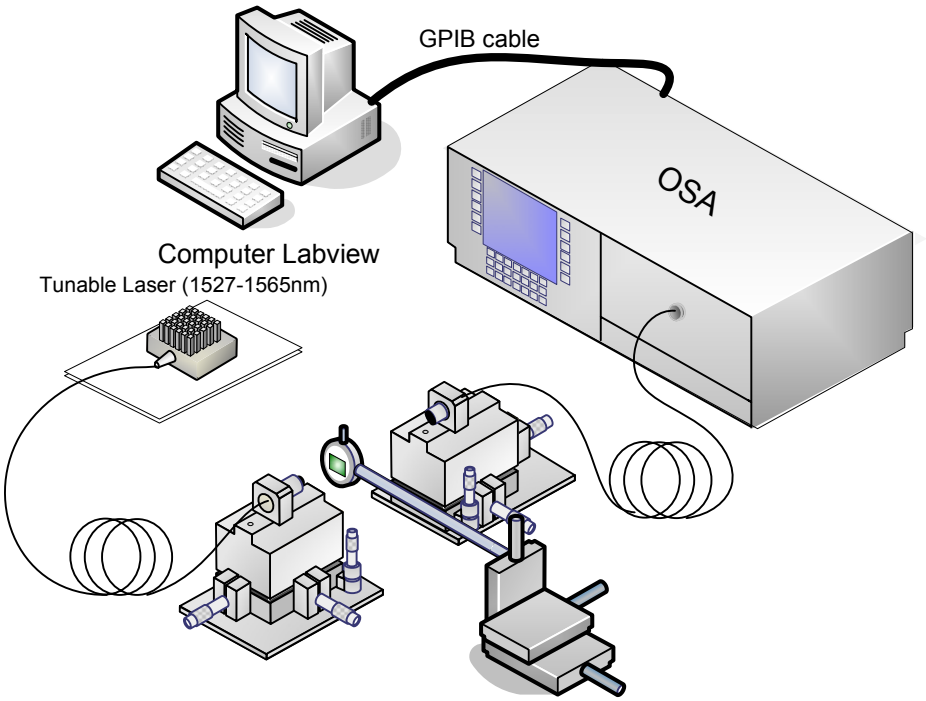

Figure 3.43 Schematic of tunable laser test for narrowband filters.

3.4.2 Labview instrument for IV test

Virtual instrument for IV test was developed for solar cell and VCSELs (Vertical Cavity Surface Emitting Lasers) test measurement. For this test, Keithley sourcemeter 2612 was used to measure IV curve for devices, and some labview codes are provided by product company which is Keithley Instruments Inc. The Keithley sourcemeter 2612 has two channels and each channel can be voltage source, current source, or digital multimeter (DMM).

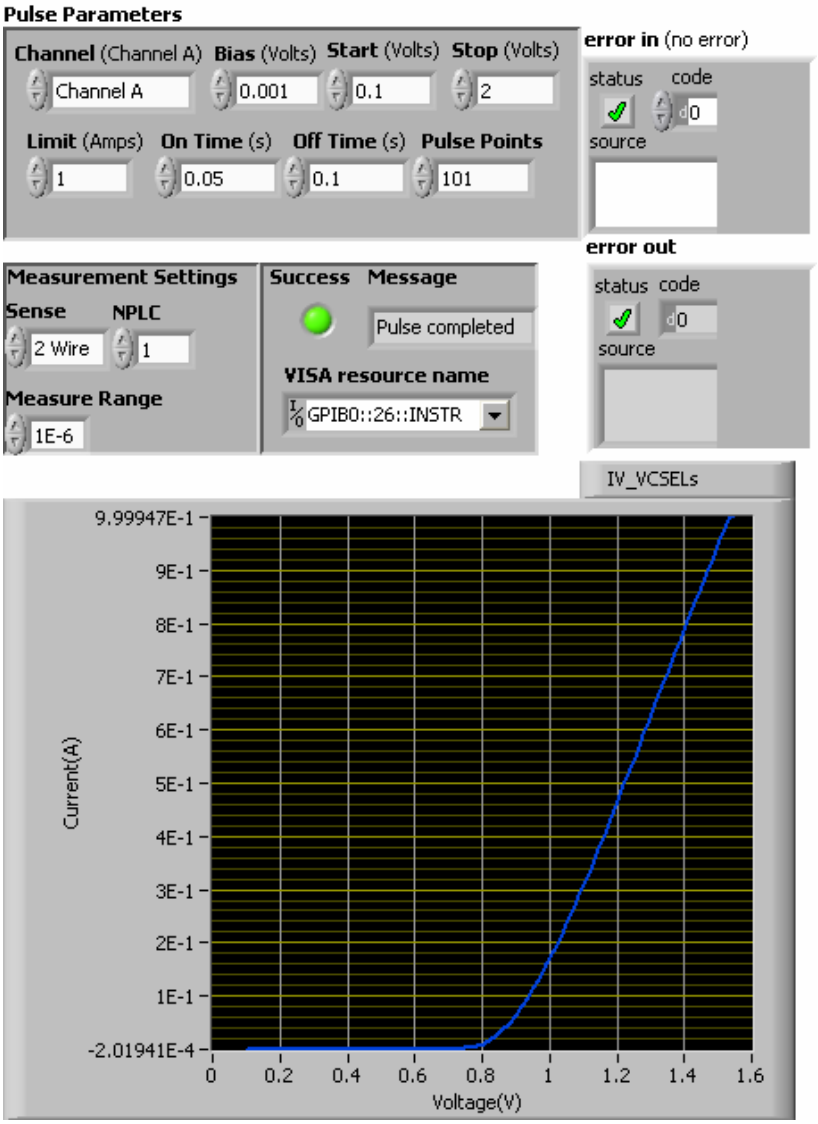

Figure 3.44 Labview for solar cell and VCSELs test.

At Front panel of this VI, some parameters can be set the details as follows: smua for channel A or smub for channel B, Bias voltage which is DC bias voltage in volts since in this VI using configuration pulsed voltage measured current sweep linear, Start which is pulse sweep start level in volts, Stop which is pulse sweep stop level in volts, Limit which is compliance current limit in amps, On times which is pulse width on-time in seconds, Off times which is pulse off time in seconds, Pulse points which is number of pulse measure cycles, Sense which can be

selected between 2-wire or 4-wire measurement, NPLC (Number of Power Line Cycles) which is the power-on speed setting corresponding to the integration time, or measurement aperture (period of time the input signal is measured) ,for example, NPLC can be set between 0.01 PLC which is the fastest integration time (obtained more noise) and 25 PLC which is the slowest integration time (obtained less noise), and the default NPLC is 1, Measure range must be set in order to get the accuracy voltage or current measurement, and VISA resource name which is specified the GPIB address for the sourcemeter connecting to the labview program.[11]

At block diagram of this VI, from Figure 3.45, the Initialize subVI is used to write the data from write buffer to the sourcemeter specified by VISA resource name, and used to read number of data in bytes from the sourcemeter or interface into read buffer. Then, VISA Write creates the table to place the buffers in for voltages and current value in IV measurement. In Error Query subVI, it is used to generate error message code when error happens in order to easily correct what is kind of this error. For Make Buffer subVI, it is used to create a RAM buffer for keeping currents and voltages into the table buftable.i (command: buftable.i = smua. makebuffer (200)) or buftable.v (command: buftable.v = smua.makebuffer (200)) in this case, channel A and number of pulse points=200 was selected. For Clear subVI, it is used to clear all reading from the indicated buffer which is buftable.i and buftable.v. For Buffer Configure subVI, the function of this subVI has four parts so called “buffer storage control attributes” as follows: First, the append modes are either off or on. When the append mode is off, a new measurement to this buffer will overwrite the previous contents. When the append mode is on, the first new measurement will be stored at what was formerly reading buffers [n+1]. This attribute is initialized to off when the buffer is created.[11] Second, collectsourcevalues is used to enable or disable source value storage when this attribute is on, source values will be stored with readings in the buffer. This requires 4 extra bytes of storage per reading. This value, off or on, can only be changed when the buffer is empty. When the buffer is created, this attribute is initialized to off.[11] Third, collect timestamps is used to enable or disable time stamp storage.

When this attribute is on, time stamps will be stored with readings in the buffer. This requires 4 extra bytes of storage per reading. This value, off or on, can only be changed when the buffer is empty. When the buffer is created, this attribute is initialized to off.[11] Last, timestamp resolution is used to set time stamp resolution of nvbuffer1 table at channel A to 0.001 second if the command is smua.nvbuffer1.timestampresolution = 0.001. The time stamp resolution, in seconds. When the buffer is created, its initial resolution is 0.000001 seconds. At this resolution, the reading buffer can store unique time stamps for up to 71 minutes. This value can be increased for very long tests. Finally, last subVI, SMU reset, is used to reset sourcemeter unit that is channel A or B.[11]

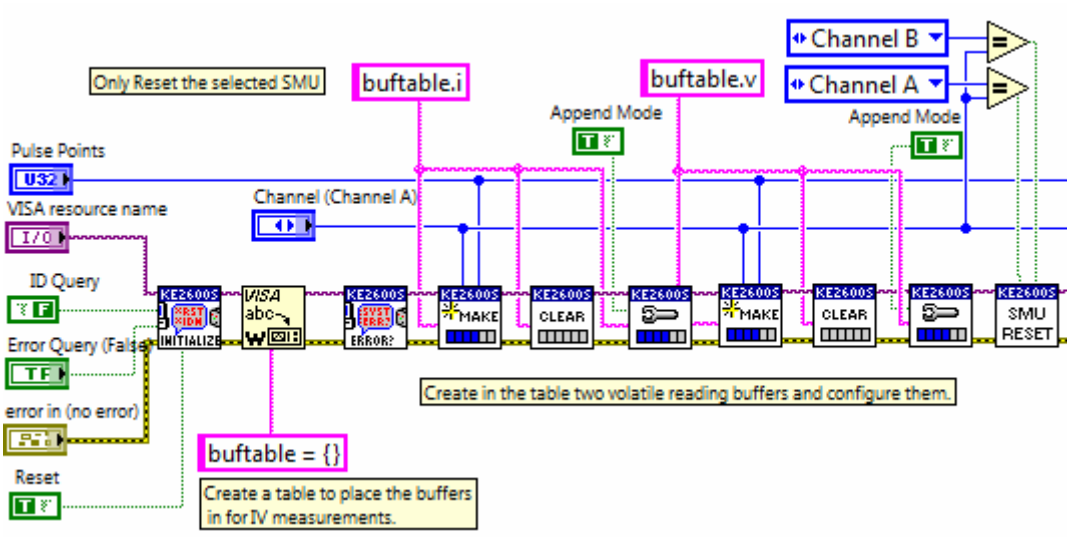

Figure 3.45 Block diagram of labview for resetting sourcemeter unit (SMU).

From Figure 3.46, for Source Function subVI, it is used to set the functions of sourcemeter either current source function or voltage source function. The commands for this function are smua.source.func = smua.OUTPUT_DCAMPS for select channel A to be a current source function and smub.source.func = smub.OUTPUT_DCVOLTS for selecting channel B to be a voltage source to be a voltage source function. For Source Autorange subVI, it is used to set auto range for current or voltage source, for example, the programming command:

smua.source.autorangei = smua.AUTORANGE_ON or smua.source.autorangei = 1 is used to enable current source (last letter before equal sign) auto range at channel A, or the command: smub.source.autorangev = smub.AUTORANGE_OFF or smub.source.autorangev = 0 is used to disable channel B voltage source range to auto. For NPLC subVI, it is the speed key used to set the integration time, for example, the command: smua.measure.nplc = 0.001 used to set NPLC= 0.001. For Measure Autorange subVI, it is used to write measure auto range, for example the command: smua.measure.autorangev = smua.AUTORANGE_ON or smua.measure.autorangev =1 used to set voltage range at channel A to auto. For Measure Range subVI, the function of this VI is to selecting manual current or voltage measure range, for example, the command : smua.measure.rangei = 0.001 used to select manual current (last letter before equal sign) measure range. For Measure Sense Mode subVI, it is used to write sense mode into channel A or B, for example, the command: smub.sense = sense, and setting sense to one of the following values: 0 or smuX.SENSE_LOCAL used to select local sense (2-wire), 1 or smuX.SENSE_REMOTE used to select remote sense (4-wire), and 3 or smuX.SENSE_CALA used to select calibration sense mode. Last, Measure Autozero subVI is used to write autozero into channel A or B, for example, the command: smua.measure.autozero = smua.AUTOZERO_OFF or smua.measure.autozero = 0 is used to disable autozero.[11]

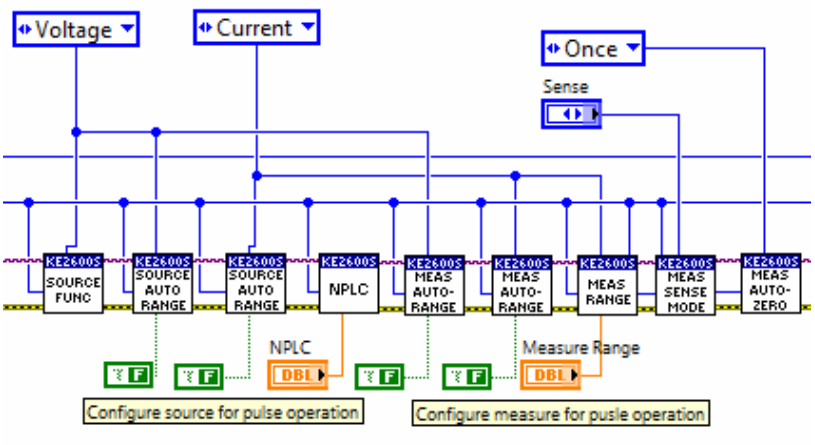

Figure 3.46 Block diagram of labview used to configure source or measure for pulse operation.

From Figure 3.47, For Config PulseVMeasureISweepLin subVI, it is used to configure a linear pulsed voltage sweep with a current measurement at each point. Measurement will be made at the end of the on-time. The magnitude of the first pulse will be start volts. The magnitude of the last pulse will be stop volts. The magnitude of each pulse in between will be step volts larger than the previous pulse where: step = (stop - start) / (points - 1) as shown in Figure 3.48.[11] The command of this function as shown below:

f, msg = ConfigPulseVMeasureISweepLin (smu, bias, start, stop, limit, ton, toff, points, buffer, tag [, sync_in][, sync_out][, sync_in_timeout][, sync_in_abort]) as shown in Figure 3.49 ,and the meaning of the parameters inside this command are as follows:

First, smu is smua (channel A) or smub (channel B). Second, bias is pulse bias level in volts since this function using sweep voltages measure current. Third, start is pulse sweep start level in volts. Fourth, stop is pulse sweep stop level in volts. Fifth, limit is compliance current limit in amps. Sixth, ton is pulse width on-time in seconds. Seventh, toff is pulse off-time in seconds. Eighth, points are number of pulse in cycles. Ninth, buffer means reading buffer where pulsed measurements will be stored. Tenth, tag means numeric identifier to be assigned to the defined pulse train. Eleventh, sync_in is used to define a digital I/O trigger input line. If programmed, the pulse train will wait for a trigger input before executing each pulse. This parameter is optional. Twelfth, sync_out is used to define a digital I/O trigger output line. If programmed, the pulse train will generate a trigger output immediately prior to the start of ton. This parameter is optional. Thirteenth, sync_in_timeout is used to specifies the length of time (in seconds) to wait for input trigger (defaults to 10s). Fourteenth, sync_in_abort is meaning (true or false) whether to abort pulse if input trigger is not received before timeout expires (defaults to true).[11]

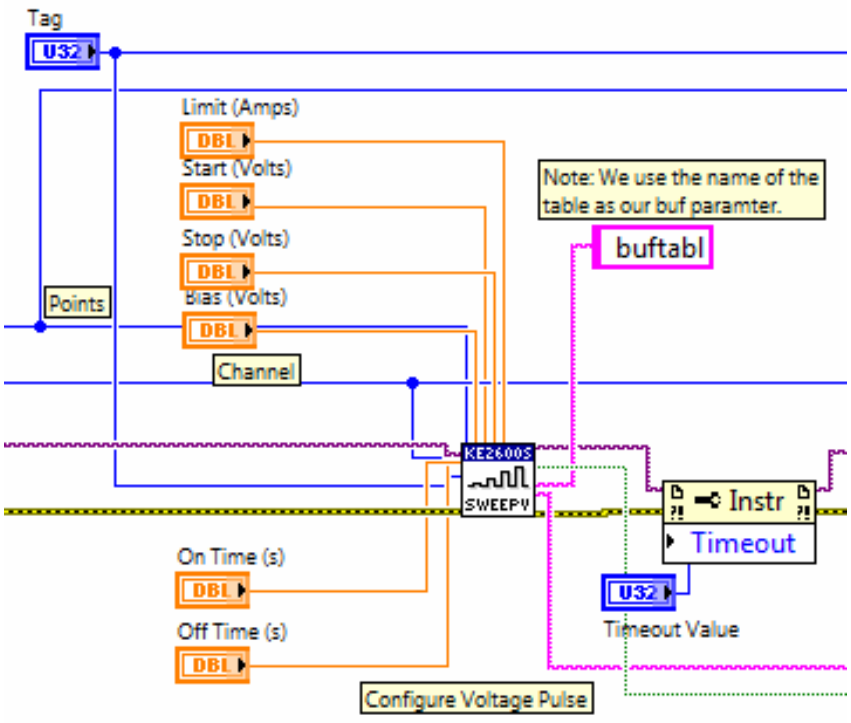

Figure 3.47 Block diagram of labview used to pulse voltage and measure current sweep.

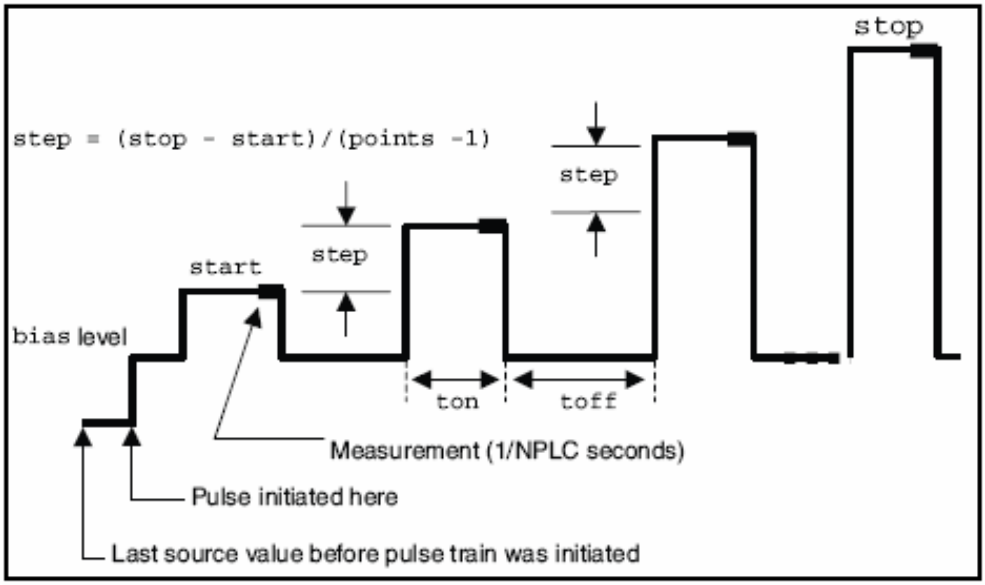

Figure 3.48 Waveform of ConfigPulseVMeasureISweepLin.[11]

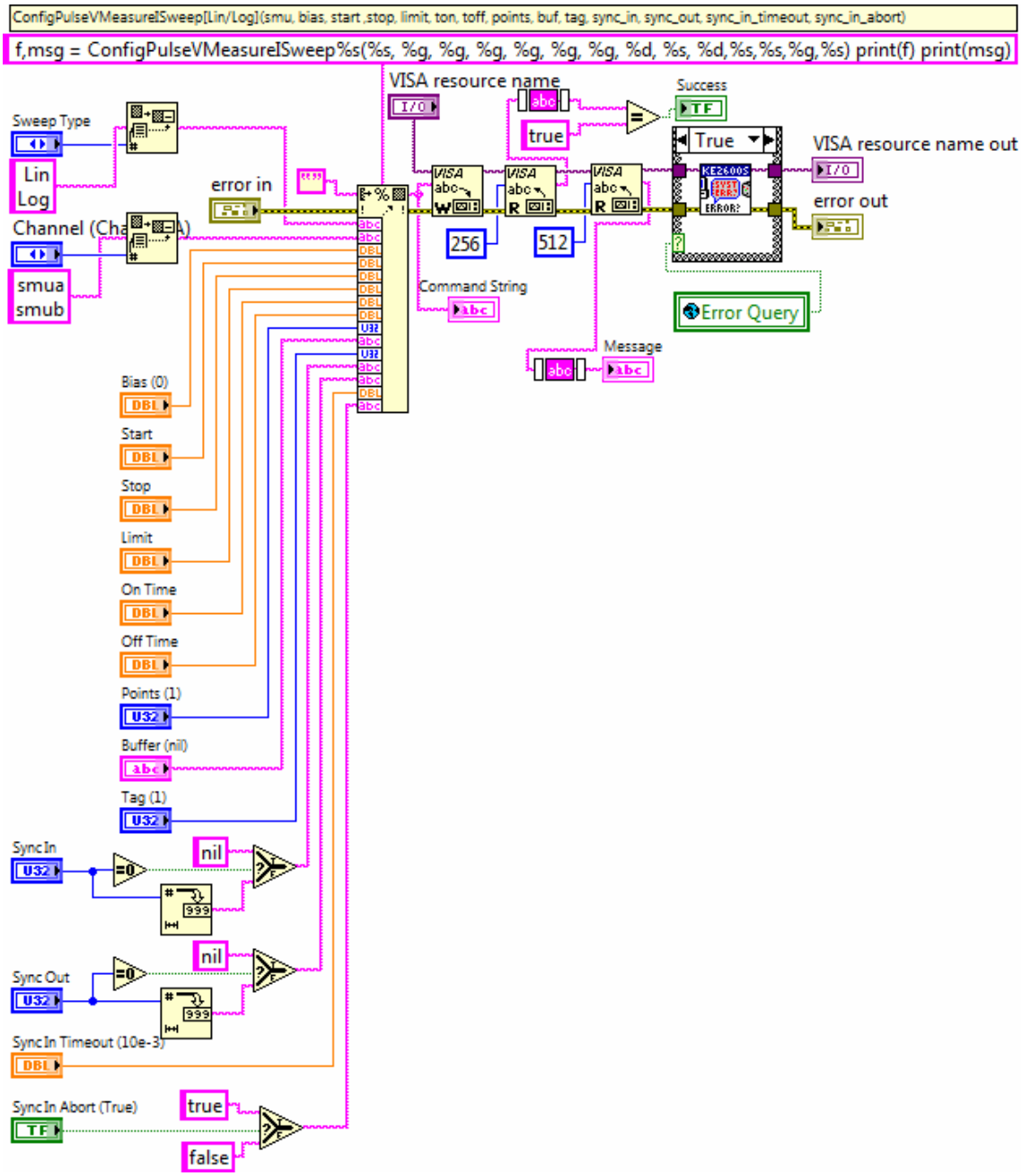

Figure 3.49 Block diagram of ConfigPulseVMeasureISweepLin subVI.

From Figure 3.50, the main function of this block diagram is turn on or off output sourcemeter and print out current and voltage from buftable.i and buftable.v respectively. For Source Output Enable subVI, it is used to turn on or off pulse test by using the command: smua.source.output = smua.OUTPUT_ON which is used to turn on output of channel A, or smub.source.output = smub.OUTPUT_OFF which is used to turn off output of channel B. For Initiate Pulse Test subVI, the main function of this subVI is used to initiate the pulse configuration assigned tag which is parameter numeric identifier of pulse train configuration to be initiated by using command: f, msg = InitiatePulseTest (tag) . For Print Buffer subVI, it is used to print data from buffer subtables, for example, printbuffer (1, 100, smua.buftable.v) is used to print data and return 100 channel A reading from buftable.v .[11]

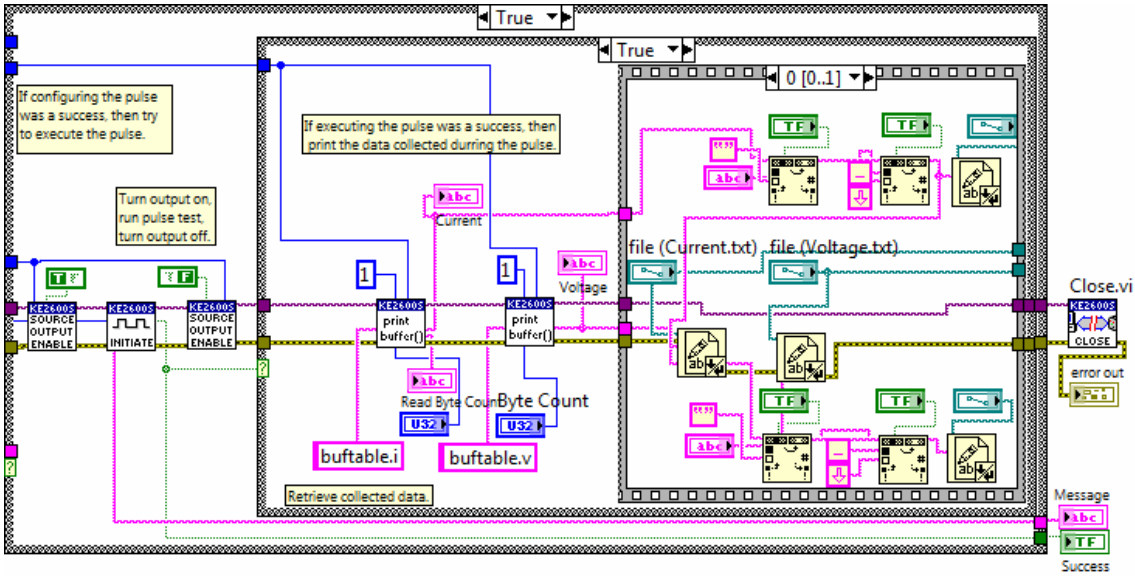

Figure 3.50 Block diagram to print currents and voltages and save in text file.

From Figure 3.51, the main function of this subVI is plotting IV curve and data will be saved in form of text file as shown in Figure 3.52.

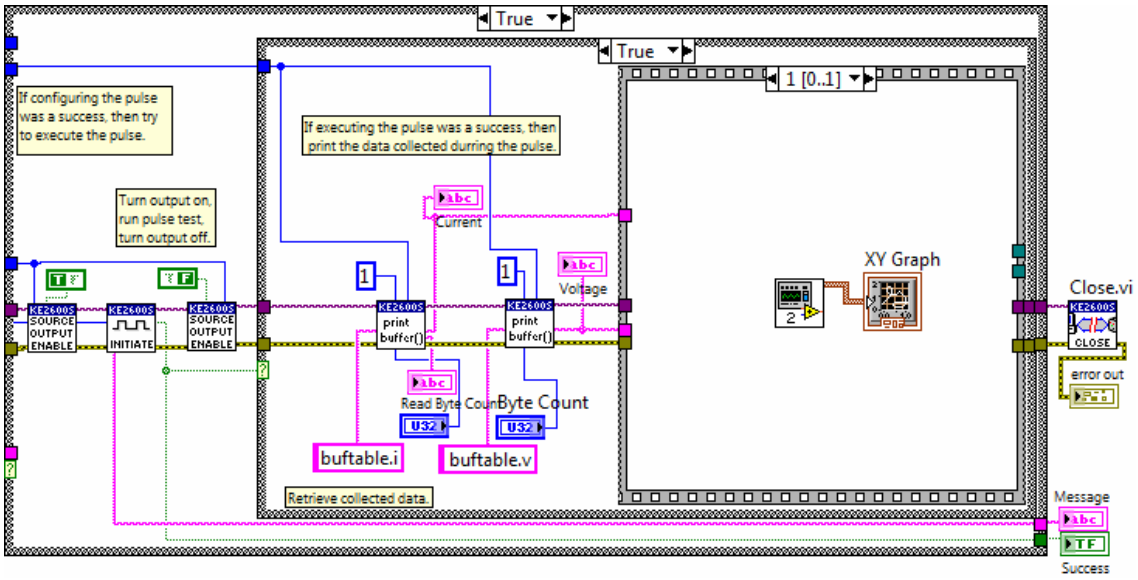

Figure 3.51 SubVI to plot graph currents and voltages.

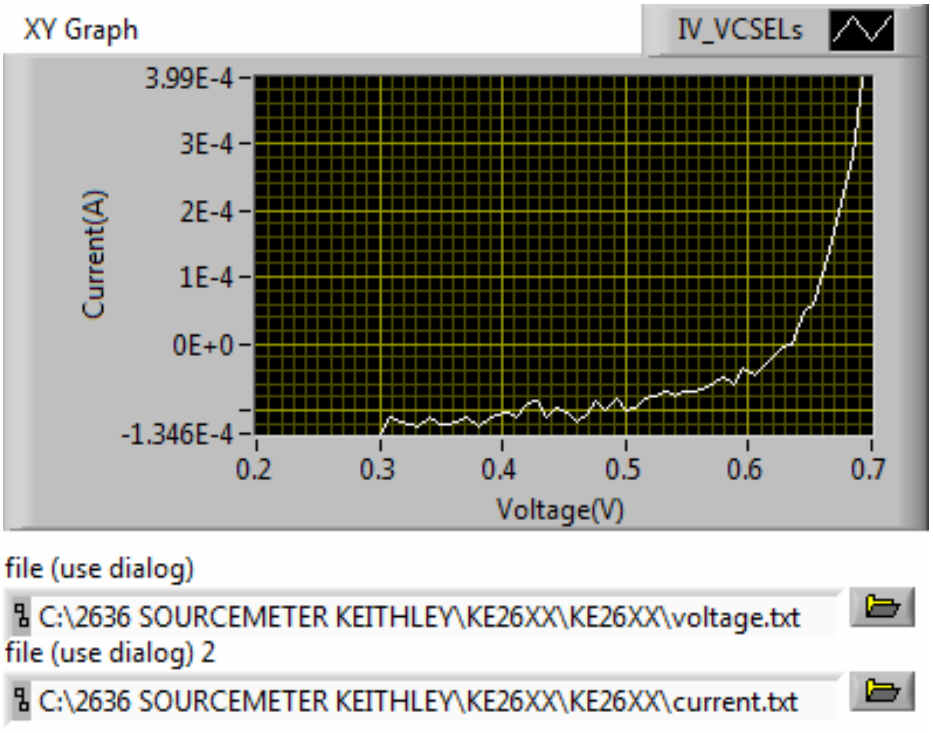

Figure 3.52 Currents and voltages plot or IV curve.

From Figure 3.53, the main function of this subVI is use to plot IV curve from text file that save in the computer. An upper line represents the voltage data and a lower line represents the current data. Then, both of such data will be put in For loop in order to plot IV curve.

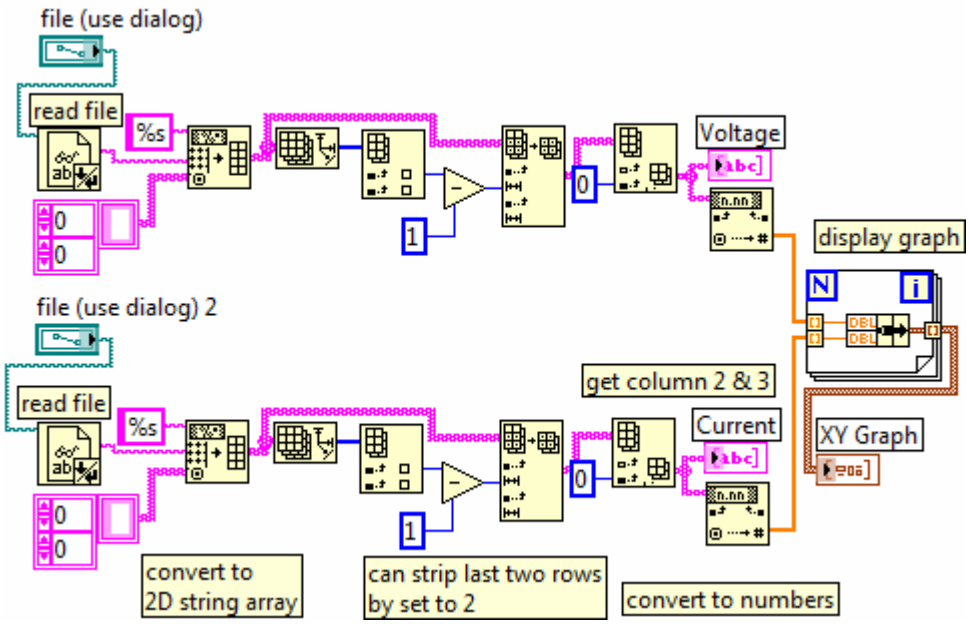

Figure 3.53 Block diagram to plot graph currents and voltages.

As shown in Figure 3.54, the results of IV curve for LabTracer program and LabView give the same plot and device which is used to test is a diode. Although Labtracer is available, it cannot use to apply for Light-Current-Voltage (LIV) test. On the other hand, Developed Labview can be applied for LIV test.

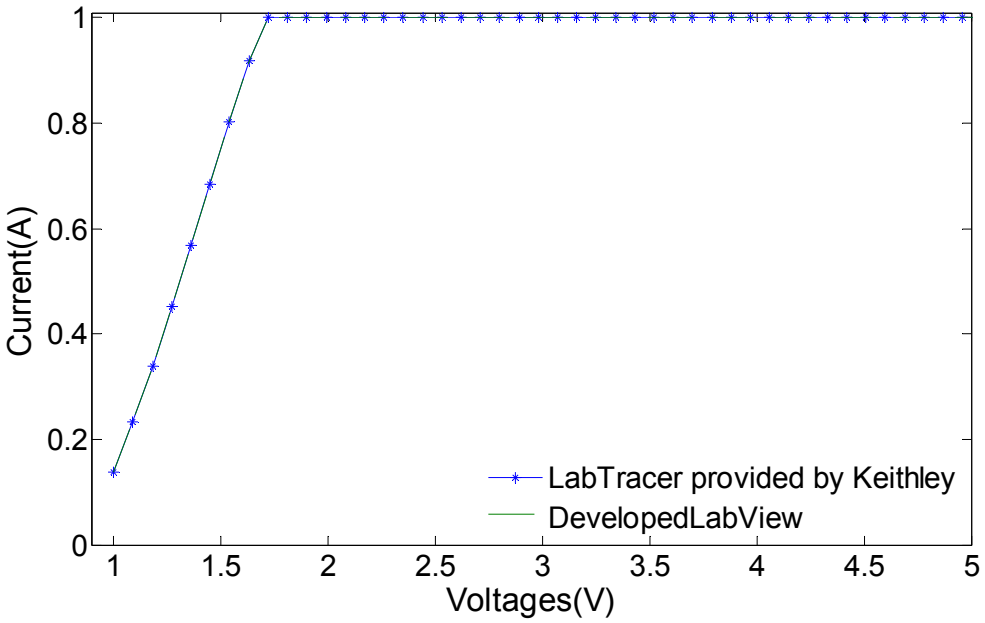

Figure 3.54 Comparison of IV curve between labtracer and developed labview.

CHAPTER 4

CONCLUSIONS

4.1 Summary

Fano resonance filters and reflectors on patterned silicon photonic crystal nanomembranes were designed with 3D-FDTD and RCWA simulations, fabricated by E-beam lithography, resonantly tuned by spectral trimming using PECVD, SOG backfill, or BHF, transferred onto glass or flexible PET substrate by using a direct wet-transfer process, and characterized by transmission and reflection measurements. The measured transmission and reflections results agree well with the designs for both narrowband filter and broadband reflector structures on foreign substrates. Further design and process optimizations can lead to high Q filters and high reflectivity broadband reflectors, desirable for ultra-compact surface normal modulators, detectors and light sources.

4.2 Future work

The advent of advanced nanofabrication or nanomembrane technology has led to the realization of compact optical filters, switches, modulators, and photodetectors with high performances proper to the photonic or electronic device integration. Based on the extremely flexible substrate, the combination of the highly multilayer SiNMs plays an important role in simplification nanofabrication techniques for highly compact photonic integration.

REFERENCES

[1] H. Yang, H. Pan, Z. Qiang, Z. Ma, and W. Zhou, Electron. Lett., vol. 44, p. 858, 2008.

[2] Zexuan Qiang, Hongjun Yang, Li Chen, Huiqing Pang, Zhenqiang Ma,and Weidong Zhou.:" Fano filters based on transferred silicon nanomembranes on plastic substrates", APL 93, 061106 (2008).

[3] H. Yang, L. Chen , S. Chuwongin, Z. Qiang, H. Pang, , Z. Ma, and W. Zhou.: 'Spectral Trimmimg of Fano Reflectors on Silicon and Glass Substrates', LEOS, 2008

[4] S. Fan and J. D. Joannopoulos, Phys. Rev. B 65, 235112 (2002).

[5] R. Magnusson and S. S. Wang, Appl. Phys. Lett. 61, 1022 (1992).

[6] Y. Kanamori, T. Kitani, and K. Hane, Appl. Phys. Lett. 90, 031911(2007).

[7] H.C. Yuan, Z.Q. Ma, M. M. Roberts, D. E. Savage, and M. G. Lagally.: 'High-Speed Strained-Single-Crystal Silicon Thin-Film Transistors on Flexible Polymers', J. Appl. Phys. 100, 013708 (2006).

[8] Yuan, H.C., Celler, G.K., and Ma, Z.: '7.8-GHz flexible thin-film transistors on a low-temperature plastic substrate', J. Appl. Phys.,2007, 102, p. 034501

[9] http://www.crystec.com/trioxide.htm

[10] Quick reference HP 71450B/1B/2B Optical Spectrum Analyzers.

[11] Keithley Instruments, Inc.:"Series 2600 System SourceMeter® Instruments Reference Manual", 2008.

[12] John D. Joannopoulos, Steven G. Johnson, Joshua N. Winn, Robert D. Meade.: "Photonic Crystals Molding the Flow of Light Second Edition", Princeton university press

BIOGRAPHICAL INFORMATION

He was born in Manorom district, located in Chainat province, Thailand 1972. He received his bachelor's degree in Telecommunication Engineering at King Mongkut's Institute of Technology Ladkrabang, one of the most famous universities in Thailand, in May 1995. He has been employed by Jasmine Telecom System Public Company Limited from May 16, 1995 to September 8, 2006. His last position is Engineering Supervisor in Payphone Business Unit.

In 2006, after he had worked for eleven years, he quit the job and decided to compete for the Royal Thai Government scholarship in an examination. In September 2006, he had been awarded the Royal Thai Government scholarship. He started studying graduate level at the University of Texas at Arlington (UTA) in 2007 to pursue his Master's degree in Electrical Engineering over the area of Silicon Photonics Crystal Project. During studying at UTA, his advisor is Prof. Weidong Zhou. After he received the Master's degree, he will continue to study PhD program in the nanotechnology area. In the near future, when he finishes the PhD degree, he will go back to his country in order to work for the National Institute of Metrology in Thailand (NIMT) and his responsibility is to develop metrology system, procure and maintain national standards and standard reference materials of the country for fields of light and color measurement, and promote careers on metrology and fortify capability of the calibration laboratory.